

A Surface EMG System Local Muscle Fatigue Detection

A Surface EMG System

Local Muscle Fatigue Detection

By

Wencong Xu

In partial fulfillment of the requirements for the degree of

Master of Science
In Electrical engineering

At the Delft University of Technology,
To be defended publicly on Wednesday, May 27, 2020, at 10:00 AM.

Supervisor:	Dr.ir. A. Bossche Prof.dr. P.J. French Ing. J. Bastemeijer MSc A.S.M. Steijlen
Thesis committee:	Dr.ir. A. Bossche Prof.dr. P.J. French Dr.ir. A. C. Schouten MSc A.S.M. Steijlen Ing. J. Bastemeijer

Abbreviations

ADC	Analog-to-digital converter
DR	Data rate
EMG	Electromyography
IMU	Inertial measurement unit
MDF/MPF	Median power spectrum frequency
MFPV	Muscle fiber propagation velocity
MNF	Mean power spectrum frequency
MUAP	Motor unit action potential
PS	Power spectrum
RPM	Rounds per minute
sEMG	Surface Electromyography
SPS	Samples per second

Contents

Contents.....	6
ABSTRACT.....	8
ACKNOWLEDGMENTS.....	9
1. Introduction	11
1.1. Background	11
1.2. History of sEMG	12
1.3. Objective	13
1.4. Structure of the thesis	14
2. Literature Survey.....	15
2.1. Skeletal muscle.....	15
2.2. Surface EMG signals.....	16
2.2.1. Generation and transmission of sEMG signals	16
2.2.2. Advantages and disadvantages of sEMG signals in detecting local muscle fatigue.....	21
2.2.3. Characteristics of raw sEMG signal.....	21
2.2.4. Noise sources and noise reduction methods.....	23
2.3. Muscle fatigue in sEMG signals	23
2.4. sEMG sensors.....	24
2.4.1. Electrode material	25
2.4.2. Effect of polarization on the electrode potential	26
2.5. ADCs.....	27
3. System Requirements and Measurement Approach.....	28
3.1. Experiment with Biosignalsplex	28
3.2. Requirements for the system	31
3.2.1. Requirements for MNF analysis	32
3.2.2. Requirements for MFPV analysis	32
3.3. Experimental requirements	34
3.3.1. The measured muscle	34
3.3.2. Isometric exercise.....	36
3.3.3. Isotonic exercise	38
4. System Design.....	40
4.1. Electrodes and input cables	41
4.2. ADCs	42
4.3. Microcontroller.....	45
4.4. Computer.....	46
4.4.1. Data collection.....	46
4.4.2. Data processing and analysis.....	47
5. Experiment and Results.....	49
5.1. The experimental procedure	49
5.2. The experimental results	51
5.2.1. Wall-sit	51
5.2.2. Isotonic exercise, cycling	60
6. Discussions and Future Works	63
6.1. Discussions.....	63
6.2. Future works.....	63
6.2.1. Improvement of system performance	63
6.2.2. Improvement of physiological experiment	64

References	65
APPENDIX-A	67
Circuit diagrams	67
APPENDIX-B	69
Protocol for the physiological experiment	69
1. Introduction and objectives	69
2. Research questions	69
3. Materials:.....	69
4. Methods	70
5. Uncertainties.....	70
6. Procedure.....	71
APPENDIX-C	75
Arduino-ESP32 source code	75
1. Pin connection	75
2. Read and write register functions.....	75
3. Serial Read 1-channel output data from ADS1299	76
4. Serial Read 2-channel output data from ADS1299	79
5. Read data to SD card.....	81
APPENDIX-D	84
Serial monitor	84
APPENDIX-E	85
Data processing	85
1. Import data	85
2. Plot samples and filtered samples	86
3. Plot power spectrum density (PSD)	87
4. Plot MNF, MDF and MFPV	87

ABSTRACT

In the last 4 decades, surface electromyography (sEMG) signal processing has been applied to detect local muscle fatigue, this non-invasive approach is suitable for detecting EMG signals generated by athletes in motion. Also, EMG could directly reveal the muscle's performance like endurance and recruitment of motor units, which is hard to be obtained by other methods. With the sEMG system, we can research whether EMG signals can be used to measure muscle fatigue and how this relates to injury risk. This thesis aims to build a sensor node for sEMG to detect local muscle fatigue.

An sEMG system is built for this purpose, and a physiological experiment is designed to collect sEMG signals from human muscle (Vastus Medialis) using the sEMG system. Both isometric and isotonic exercises are studied. The data analyzing method is calculating mean power spectrum frequency (MNF), median power spectrum frequency (MDF), and muscle fiber propagation velocity (MFPV) of the collected sEMG signals, because local muscle fatigue is related to MNF/MDF decrease and MFPV decrease. 5 groups of isometric exercise, wall-sit and 2 groups of isotonic exercise, cycling, are recorded. All the athletes are healthy males, around 25. The data analyzing result shows that MNF/MDF decrease is related to muscle fatigue, and MFPV changes similarly with MNF/MDF.

ACKNOWLEDGMENTS

I would first like to thank my supervisors, Dr.ir. A. Bossche, Prof.dr. P.J. French, Ing. J. Bastemeijer, MSc A.S.M. Steijlen, without whom I would not have been able to complete this thesis project.

My direct supervisor, Dr.ir. A. Bossche has introduced me to this thesis project. His guidance helped me in all the time of research and writing of this thesis, his patience and rigorous attitude made me want to do better and keep learning.

Prof.dr. P.J. French gave me many pieces of important advice, including the improvement of physiological experiment setup and thesis report content, etc. His advice about the experiment setup made my results more convincing.

Ing. J. Bastemeijer helped me a lot with hardware design, software design and writings. It was the first time that I built a sensor system like this, his guidance was so important for me to get through the system design.

MSc A.S.M. Steijlen gave me many helpful suggestions on the experiment design and writings. I could feel myself in progress whenever I discuss with her about the design ideas and writings. I really appreciated her for spending a lot of time on helping me improve my report and system.

And I would like to thank the voluntary subjects who participated in the physiological experiments. They were my colleagues and my friends, they also discussed with me about my project and gave me many useful pieces of advice.

I would also like to thank the staff members of the X TU Delft sports center, who precisely supported us in physiological experiments. With their permission for us and the athletes to use exercise equipment in the gym, we could conduct experiments conveniently and less expensively.

My last words come to my family. They constantly supported me by sharing my mood and details of my life through the phone. And I would never forget the days when my mother came over, we had so much fun visiting the Christmas market, admiring paintings in Amsterdam, cycling in the old town of Delft. They have always inspired me.

Wencong Xu
Delft, May 2020

1. Introduction

1.1. Background

Participating in sports regularly is beneficial for health, in the Netherlands, there are about 7 million active sports participants. Safety is important for doing physical activities and sports regularly as well as keeping a healthy and strong body. However sports injuries have been one of the most common injuries in modern society, and it is often time-consuming, expensive, and difficult to treat sports injuries. Millions of sports injuries happen per year in the Netherlands, 50% of these had to be treated medically, all direct and indirect costs account for over 3,000,000,000 euro's [1] and thus, scientists are searching for preventive strategies and activities.

To build a successful and efficient sports injury prediction and prevention system, valid intervention data like human biosignals need to be collected and analyzed timely. A variety of biosignals could play a role in this system, such as electrocardiography (ECG), electroencephalography (EEG), electromyography (EMG), respiration, blood gas, blood pressure, temperature, etc. Figure 1.1 illustrates these biosignal sensors and their application on the human body.

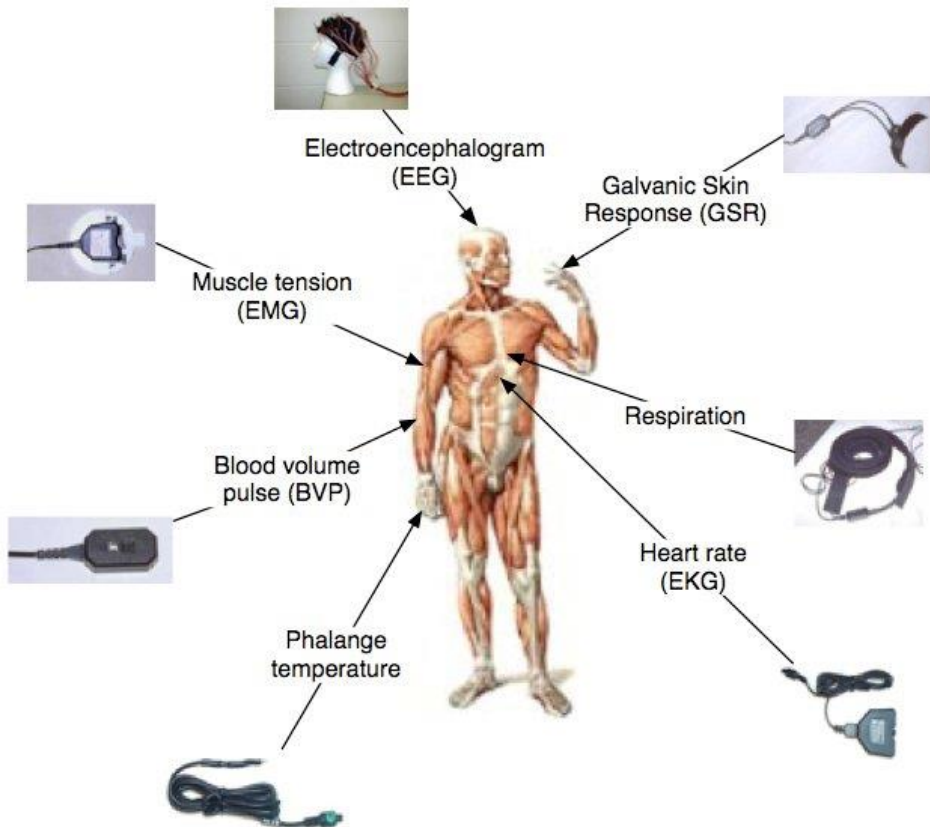


Figure 1.1 Human body biosignals [2]

An electrogram is a tracing of electric events in living tissues (such as the muscle, brain, or heart) [3]. It is usually made utilizing electrodes on the tissues. Electrocardiogram (ECG or EKG[4]), electroencephalogram (EEG), electromyogram (EMG), electrooculogram (EOG) are electrograms.

Since surface-EMG (sEMG) could directly reveal muscle's performance like work-rate, signal amplitude, and frequency, sEMG systems have been widely used in various applications. For example, surgery, physical therapy, risk prevention, and movement analysis. Correspondingly, the sEMG system components, electrodes, amplifiers, Analog-to-digital converters (ADCs), have been developed to fulfill the requirements of an sEMG system.

Bioelectrical signals (EEG, ECG, EMG, etc.) are one type of physiological signals that can be used to analyze performance. In this project, a surface EMG (sEMG) detecting and recording system is designed to study muscle fatigue. With such an sEMG system, scientists could study the influence of muscle fatigue on sports injuries.

This report is written to researchers who are interested in sEMG and its applications. I assume that the reader knows basic electronics theory and basic physiology.

1.2. History of sEMG

The early development of EMG was related to the discovery of electricity. The first written document about the bioelectric phenomenon is an ancient Egyptian hieroglyph of around 4000 B.C. describing the electric eel, which is long before the knowledge of electricity started to evolve. However bioelectric phenomenon only has had scientific value since 200 years ago.

Luigi Galvani is the discoverer of animal electricity. In around 1780, he proposed the neuroelectrical theory. In the 1780s and 1790s, he investigated the effect of electrical stimulation on dissected animals[5]. Galvani's most famous work, the *De Viribus Electricitatis in Motu Musculari Commentarius* was written in 1791, this book contained his 11 years of work on animal electricity, and it has been recognized as the beginning of modern electrophysiology.

In the 19th century, many fundamental theories of bioelectricity had been established. In 1843, Du Bois-Reymond discovered the action potential of a nerve impulse[6], and in 1890 the voluntary muscle contraction was first recorded by Marey, he introduced the term 'electromyography'.

In around 1901, Willem Einthoven (21 May 1860 – 29 September 1927, a Dutch doctor and physiologist) invented the first practical ECG, the string galvanometer[6], which is a necessary breakthrough in the foundations of neurophysiology. Figures 1.2 and 1.3 show the famous equilateral triangle which is conceived by Einthoven. It represents a triaxial bipolar ECG system, RA is electrode placed on the right arm, LA represents the left arm and LL is the left leg. The right leg is set as the ground in this 3-lead ECG system, Right Leg Electrode removes the artifact.

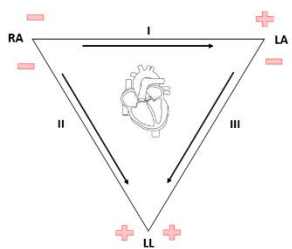


Figure 1.2 The polarity of three Standard Limb Leads [7]

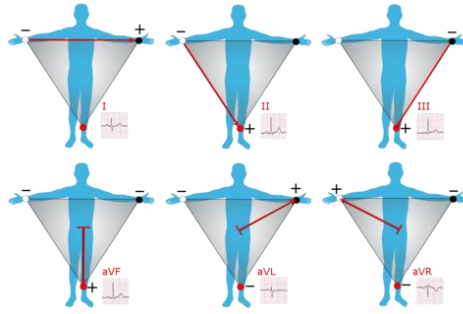


Figure 1.3 3-lead ECG [8]

In 1922, Gasser and Erlanger used an oscilloscope to display the electrical signals from muscles. The oscilloscope was modified to run at low voltages, figure 1.4 is a simplified diagram of the electron oscillograph. This contribution won them the Nobel Prize in Medicine or Physiology in 1944. Before this, the only way to measure neural electrical activity was the electroencephalograph, while it could only display large scale electrical activities.

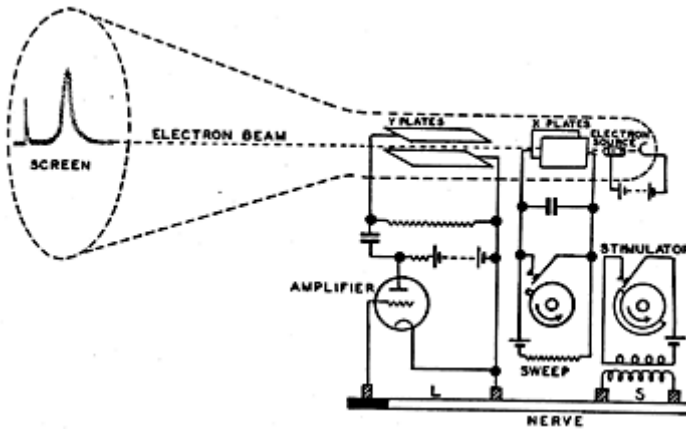


Figure 1.4 Simplified diagram of the electron oscillograph [9]

1.3. Objective

The objective of this thesis is to build a surface EMG measuring and analyzing system, which detects local muscle fatigue. The focus will be achieving a high data rate and high fidelity of the measured sEMG signals, the required data rate, and fidelity will be further explained in this section. After the system is built, it will be used in an experiment to collect sEMG data and then the data will be analyzed.

The data rate is related to frequency domain signal analysis and muscle fiber propagation velocity (MFPV) analysis, which is in the time domain. So considering the characteristics of the sEMG signals, the data rate should exceed 8,000 samples per second (SPS) for calculating MFPV, and higher sampling frequency could reveal more information of the sEMG signals in frequency domain analysis, so the sEMG sampling rate should be as high as possible.

High fidelity is necessary because the accuracy of analysis results is dependent on the quality of sEMG signals that the system records. So combining the characteristics of sEMG signals,

the signal resolution should exceed 12 bits, besides, the noises like 1/f noise, white noise, 50 Hz interference from AC main should be minimized to keep the signal as clean as possible.

1.4. Structure of the thesis

Chapter 2 will introduce the related theories including muscle physiology, sEMG signals, and the presence of muscle fatigue in sEMG signals.

Chapter 3 will discuss what the system will achieve and the system design considerations. To detect local muscle fatigue in sEMG signals, there are requirements for the collected sEMG signals.

Chapter 4 will illustrate how the system is designed in detail. Including all the hardware, software, and firmware. The important system settings are explained.

Chapter 5 will describe the experiment and its results. The experiment includes isometric exercise and isotonic exercise to collect sEMG signals from vastus medialis muscle. Mean and median power spectrum frequency will be analyzed for all the experiments.

Chapter 6 shows the discussions of the whole project and suggestions for future works.

2. Literature Survey

Human muscles can be divided into three types: skeletal muscle, cardiac muscle, and smooth muscle. sEMG signals are measured above skeletal muscles. In this chapter, firstly the structure of skeletal muscle is introduced, then the generation and transmission of EMG signals, also the advantages and characteristics of sEMG signals are introduced. Finally, the methods for identifying muscle fatigue in sEMG signals are discussed.

2.1. Skeletal muscle

Figure 2.1 shows muscle structure at different scales. From the left side to the right side of figure 2.1, the muscle structure scales down. A group of skeletal muscle contains a lot of muscle bundles, each muscle bundle is made of many muscle fibers. The tissue fascia contains contractile elements and separates muscle into layers and groups.

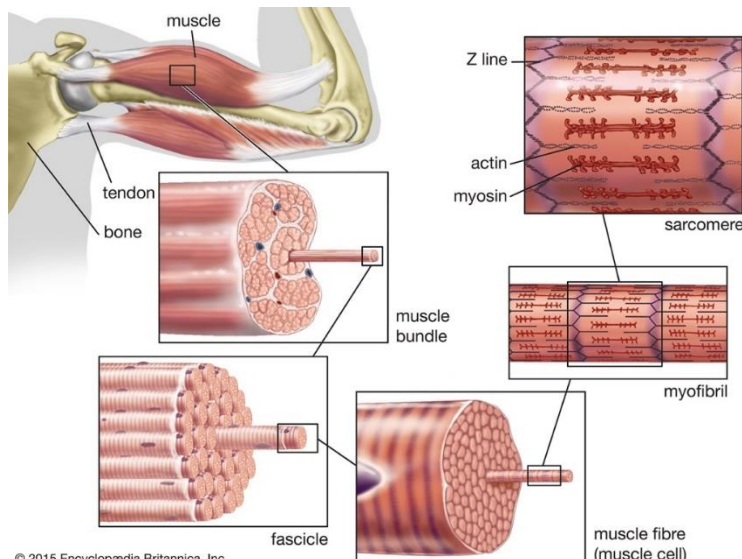
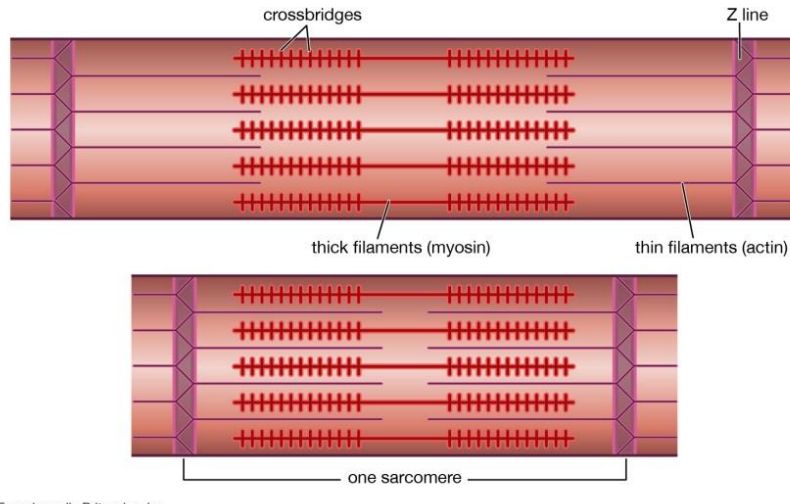


Figure 2.1 Muscle structure [10]

A contractile element is made up of many filaments in parallel and many sarcomeres in series[11]. Filaments and sarcomeres can be seen in figure 2.2. A contractile element is the part of the muscle that generates the tension, and it is this part that lengthens and shortens as negative or positive work is done.

The upper diagram of figure 2.2 shows the extended sarcomere and the lower one the contracted sarcomere. The thick filaments are $1.6\mu\text{m}$ long in vertebrate striated muscle.



© Encyclopædia Britannica, Inc.

Figure 2.2 Sarcomere structure in a striated muscle [12]

It is at the cross-bridge that tension is created, and the lengthening or shortening takes place. Cross-bridge is the structure between actin and myosin, as shown in figure 2.1 ‘sarcomere’. The length of the sarcomere is the distance between the Z lines, it can vary from $1.5\mu\text{m}$ at full shortening to $2.5\mu\text{m}$ at resting length to about $4.0\mu\text{m}$ at full lengthening.

2.2. Surface EMG signals

Electromyography (EMG) is an electrodiagnostic medicine technique for recording and evaluating the electrical activity produced by skeletal muscles. [13] Surface electromyography (sEMG) records muscle activity from the surface above the muscle on the skin.

2.2.1. Generation and transmission of sEMG signals

2.2.1.1. Sources of biopotentials

There are many different types of cells (figure 2.3) in the human body, like blood cells, gland cells, bone cells, nerve cells, muscle cells, etc. Most nerve cells and muscle cells are excitable cells. Biopotentials are produced by ions (K^+ , Na^+ , Cl^-) flow inside or outside these excitable cell membranes.

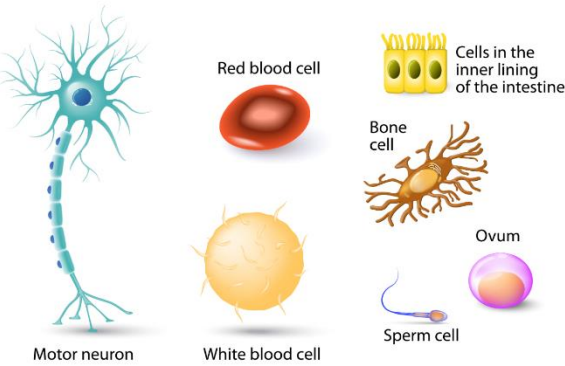


Figure 2.3 Human cell [14]

2.2.1.2. Excitation of neurons and muscle cells

A nerve cell, as shown in figure 2.4, is excited by neurotransmitter (acetylcholine, ACh) that is released by synapse of another neuron. When a neurotransmitter is detected by receptors on the dendrites, an action potential is generated on the membrane.

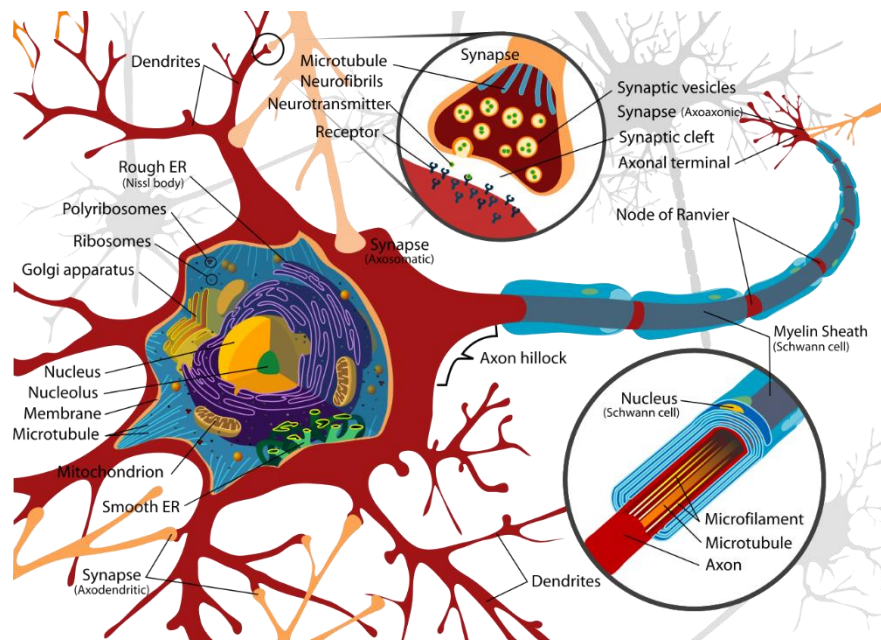


Figure 2.4 Structure of Neuron [15]

Muscles are the terminal output of the brain, muscle cells are controlled by neural cells. A motor neuron excites a skeletal muscle cell by releasing neurotransmitters (acetylcholine, ACh) to the cell membrane of muscle fiber (sarcolemma). The excitation of the muscle cell is shown in figure 2.5, figure 2.6 depicts the structure of the muscle cell.

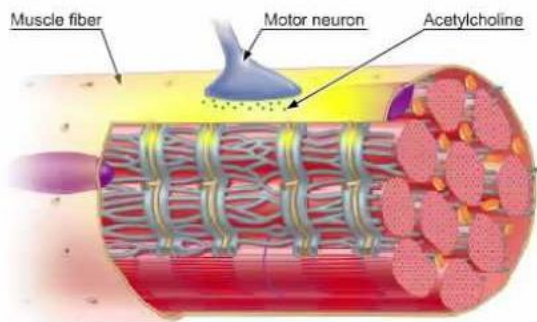


Figure 2.5 Excitation of muscle cell [16]

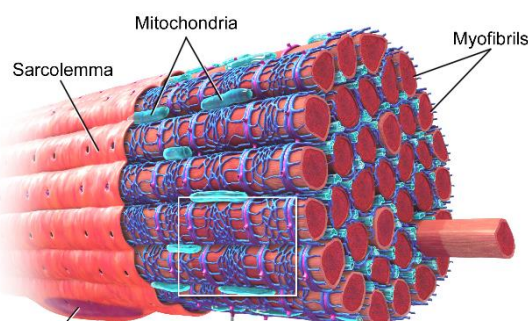


Figure 2.6 Muscle cell structure [17]

Myoelectric signals are potential variations of muscle fiber membranes. When neural control excites muscle fibers at the neuromuscular junction, which is formed by an alpha motor neuron and muscle fiber, an endplate potential (EPP) is created. Usually, it reaches a threshold level and the sarcolemma will generate an action potential, telling the proteins inside this cell to do contraction.

All muscle cells in one motor unit act simultaneously, the recruited motor units vary as the required power differs. The *size principle* [18] interpreted that, the recruitment of motoneurones (MNs) and motor units are orderly according to their sizes or tensions, the smallest motor units are recruited first, then a second, a third, etc. The largest motor unit is recruited last.

2.2.1.3. Propagation of biopotential on neuron membranes

As shown in figure 2.7, when a neuron is excited, action potential propagates from dendrites on the neuron body through the axon with myelin sheath to the synapse.

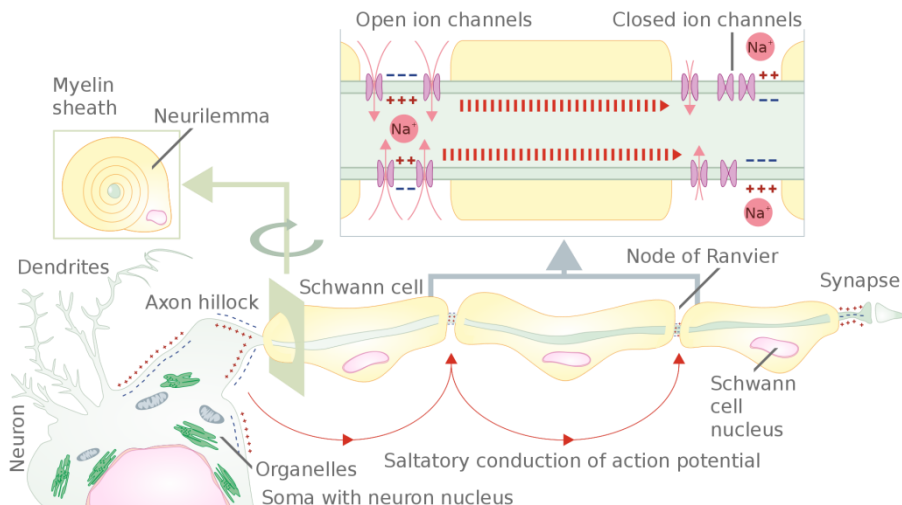


Figure 2.7 Propagation of action potential [19]

One-way propagation

The propagation is one-way because, at the repolarization zone, the ion channels cannot be activated. So, an action potential can only propagate to the adjacent zone that is at resting potential.

Effect of the myelin sheath

The axon with myelin sheath propagates action potential quicker because the membrane can only be activated at the node of Ranvier.

Chemical signal ↔ electrical signal conversion

At the synapse, the electrical signal is converted to a chemical signal and the neurotransmitter (acetylcholine, ACh) is detected by the receptors on the dendrites of the next cell, where the chemical signal is converted to an electrical signal again and the action potential continues to propagate on its membrane.

When the membrane is excited or returning to the resting state, the difference between intracellular potential and extracellular potential changes.

The membrane (figure 2.8) is made out of two layers of phospholipid molecules, with phospholipid acid heads that are hydrophilic and two fatty acid tails that are hydrophobic, this allows the membrane to be formed in the fluid. Meanwhile, there exist many kinds of proteins on the membranes, some of them act as protein channels that allow materials to go in and out of the cell.

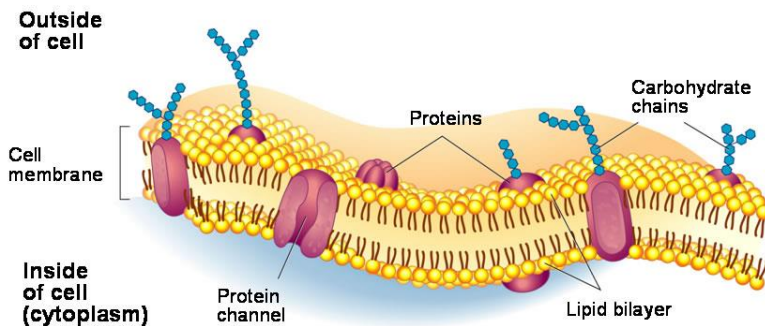


Figure 2.8 Cell membrane [20]

The flow of ions through the membrane depends on (1) the membrane permeability (2) the ratio of intracellular and extracellular concentrations and (3) the membrane voltage.

- (1) The membrane permeability of ions is voltage-dependent.
 - When the ion channels are closed, they are at the resting potential ($V_m = -90\text{mV}$) and activatable.
 - When $V_m = -60\text{mV}$, it reaches the threshold, an action potential is generated, depolarization occurs. Ion channels are opened and, Na^+ , K^+ , and Cl^- ions, etc. flow through the membrane.
 - When potential reverses, repolarization occurs, the ion channels are closed and inactivated.
- (2) The ratio of intracellular and extracellular concentrations changes when ions flow through membranes.
- (3) The membrane voltage is $V_m = \Phi_i - \Phi_o$, Φ_i is the intracellular potential and Φ_o is the extracellular potential.

Since K^+ are the main ions involved in resting state, Nernst equation can be used to calculate a reasonable approximation of membrane equilibrium potential (resting membrane). The

equilibrium occurs when the diffusion and drift of ions across the membrane reach the balance. Nernst equation at body temperature (37°C) is shown in (2.1).

$$E_k = \frac{RT}{nF} \ln \frac{[K]_o}{[K]_i} = 0.0615 \log_{10} \frac{[K]_o}{[K]_i} \quad (V) \quad (2.1)$$

Here E_k is membrane voltage, which is the potential difference between intracellular and extracellular potential, $E_k = V_i - V_o$. R is the universal gas constant, T is the absolute temperature in K, n is the valence of K^+ , F is Faraday constant. $[k]_o$ is the extracellular concentration of K^+ in (mol/L), $[k]_i$ is the intracellular concentration of K^+ in (mol/L).

Considering the influence of Na^+ and Cl^- , a more accurate expression for membrane equilibrium potential can be obtained by the Goldman–Hodgkin–Katz voltage equation

$$E = \frac{RT}{F} \ln \left\{ \frac{P_K[K]_o + P_{Na}[Na]_o + P_{Cl}[Cl]_i}{P_K[K]_i + P_{Na}[Na]_i + P_{Cl}[Cl]_o} \right\} \quad (V) \quad (2.2)$$

At steady state (1 Resting potential in figure 2.9), the intracellular potential is about -70 mV to -90 mV (negative resting potential) lower than the extracellular potential due to ion pumping. At active state, Na^+ ions flow into the cell, while less K^+ ions flow out of the cell, causing a membrane depolarization (2 Peak action potential in figure 2.9), the positive active potential is up to +30 mV. The depolarization will be immediately restored because of the diffusion characteristic of muscle fiber membrane, Na^+ ions flow out and K^+ ions flow in, and the membrane potential comes back to -80 mV (5 in figure 2.9), the repolarization.

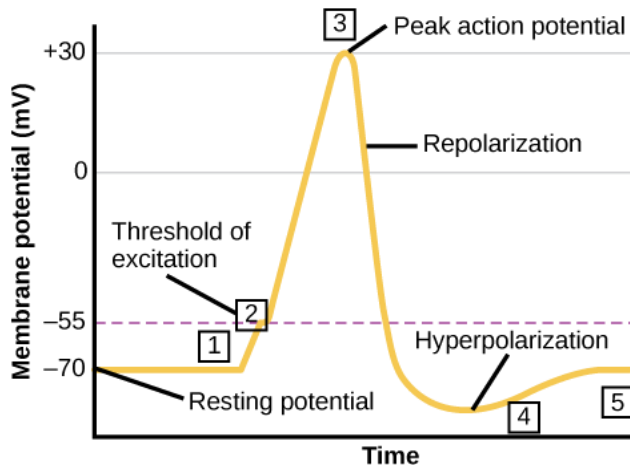


Figure 2.9 Depolarization and repolarization of the membrane [21]

2.2.1.4. Transmission of EMG from the cell membrane to the electrodes

sEMG signals are detected through multiple electrodes on the skin. Potential variations of the membrane are transmitted through connective tissue and skin to the electrodes. Connective tissue can be both in series and in parallel with the contractile element. An individual Motor Unit Action Potential (MUAP) detected through an electrode is dependent on the size of the motor unit, the distance from the motor unit to the electrode, and the tissue type in between.

When the size of the motor unit increases (Milner-Brown and Stein, 1975), or the distance decreases, the detected potential increases.

2.2.2. Advantages and disadvantages of sEMG signals in detecting local muscle fatigue

2.2.2.1. Advantages

Compare the sEMG sensor with the other methods like chemical sweat sensor or Inertial measurement unit (IMU) sensor, which are related to detecting fatigue, it has several important advantages.

- First, it enables researchers to directly "look" into the muscles: Myoelectric signals are detected, which are formed by potential variations of muscle fiber membranes.
- Second, it allows researchers to measure muscular performance: work-rate, signal amplitude, frequency, etc. some of which are useful factors for fatigue analysis.
- Third, it allows researchers to analyze to improve sports activities.
- Fourth, it detects muscle response in ergonomic studies. And with the development of interdisciplinary, more applications of the sEMG signal is going to be found.
- Also, there are some differences between EMG and sEMG. Compared to the EMG recorded from indwelling electrodes, sEMG is more reliable, researchers have compared the test-retest reliability of sEMG and needle EMG in the deltoid muscle, the average reliability for sEMG is 0.88 and for indwelling EMG is 0.62 [22]. Also, the number of associated motor units in the pick-up zone of the sEMG electrode is considerably larger. Also, sEMG is easier to be applied and more comfortable for the subjects of study.

2.2.2.2. Disadvantages

- To collect sEMG signals from human muscles, electrodes are placed on the skin. It is complex and time-consuming to do skin preparation and apply electrodes to the human body. And the positions of electrodes are different for everyone.
- Wet electrodes are commonly used for sEMG measuring, however, the viscosity of wet electrodes could be reduced by sweat. When the electrodes become not sticky, they may move on the skin or fall.
- Compared to the other sensors like chemical sweat sensors or IMU, the sEMG measuring system transfers much larger amounts of data per second to the processor.

2.2.3. Characteristics of raw sEMG signal

A raw sEMG signal is an unfiltered and unprocessed sEMG signal. Its quality can be affected by the amplifier, the detecting condition, the environmental noise. The baseline noise should not exceed 3-5 mV, the default value is 1-2 mV.

The frequency range of ECG, EEG, EMG signal, and noise distribution are shown in figure 2.10, raw EMG signal is lying in 20 Hz to 1000 Hz frequency range.

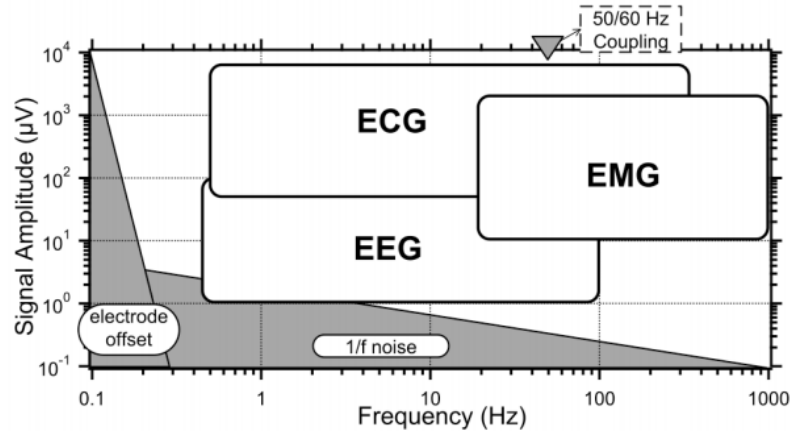


Figure 2.10 Biopotential signal frequencies [23]

Raw sEMG signals are detected through the electrodes placed on the skin that is above the muscle. As shown in Figure 2.11, the detected sEMG signal is the superposition of EMG signals generated by different motor units.

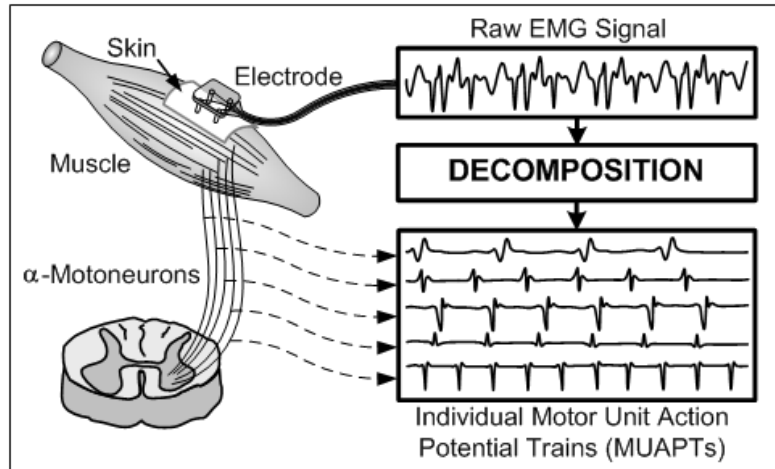


Figure 2.11 Raw sEMG signal shows associated MUAPs superposition [24]

Figure 2.12 shows the components of a MUAP, the horizontal axis is time and the vertical axis is potential. The terminal phase is the phase of the Terminal part. The terminal part is produced during dying out of the depolarized zones of sarcolemma at the ends of the fibers [25].

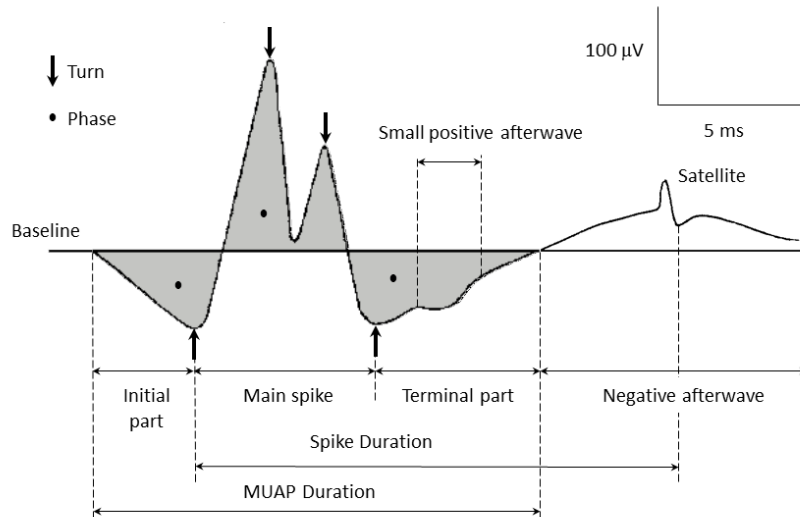


Figure 2.12 Parts of the MUAP [26]

2.2.4. Noise sources and noise reduction methods.

Noises like 1/f noise, power line noise, and the cable motion artifact, movement artifact, baseline noise could affect the sEMG signals.

a) 1/f noise.

Doing digital filtering to the raw sEMG signal could reduce 1/f noise.

b) The power line noise.

50Hz AC main noise in Europe is reduced by a reference electrode in the sEMG system, and the system is powered by battery only. The cable motion artifact can be reduced by proper circuit design. Also, a digital notch filter at 50 Hz is applied to the raw sEMG to further reduce the power line noise.

c) Movement artifact noise.

Muscle movements relative to the skin during exercises cause the movement artifact noise. The muscle fiber propagation velocity analysis is affected because the signals are sensed on the skin rather than in the muscle. Doing isometric exercise could reduce the influence of this type of noise.

d) Baseline noise.

The baseline noise is formed by the thermal noise in the amplification system and electrochemical noise at the skin-electrode interface. It can be reduced by digital filtering.

2.3. Muscle fatigue in sEMG signals

To determine the degree of muscle fatigue, the sEMG parameters like work-rate, sEMG signal amplitude, Muscle fiber propagation velocity (MFPV), and frequency characteristics are studied. MFPV decreases when there is muscle fatigue, MFPV might be influenced by the ability of muscle fibers to uptake Calcium ions back into the sarcoplasmic reticulum. And opinions agree that the decrease of MFPV leads to mean frequency/median frequency shift of

sEMG power spectrum (PS) towards lower values. But the relationship between MFPV and PS of sEMG is not linear [25]. Some other factors are influencing PS of sEMG.

An index of fatigue is the median frequency (MDF) of sEMG, MDF is the frequency value dividing the spectrum into two halves [27]. Median power frequency shifts towards the lower frequency of the sEMG power spectrum. However, there exist some exceptions, for a patient with carnitine deficiency (a metabolic muscle disease that interferes with the processing of fats for energy production [28]), the frequency shift of MDF could be towards higher frequencies because of recruitment of type II muscle fibers [29]. Besides MDF, the mean frequency (MNF) of the spectrum has also been used as a fatigue index [30].

2.4. sEMG sensors

sEMG sensors are electrodes attached to the skin. There are 3 types of electrodes, the wet electrodes, dry electrodes, and insulating electrodes. The most commonly used sEMG electrodes are wet electrodes, however dry electrodes, and non-contact electrodes also have some advantages and may be suitable for some situations.

For wet electrodes, different types of materials are used: Ag/AgCl, AgCl, Ag, Au, etc. to provide low noise skin-electrode contact. Ag/AgCl electrodes are most commonly used.

For dry electrodes, they use no electrolyte between electrodes and skin. Electrodes are made of benign metal such as stainless steel.

For insulating electrodes, there is no direct current flow through the electrode-skin interface. The electrode just serves as a capacitor. The electrodes consist of a metal (or semiconductor) that is covered with a thin dielectric surface layer contacting the skin so that the biopotential signal is coupled from the skin to the substrate.

In Table 2.2, some dry and insulating electrodes with construction and findings are listed.

Table 2.1 Summary dry and insulating electrodes [31]

Year	Reference	Dry	Ins.	Construction	Findings
1995	Taheri		•	Si_3N_4	High signal-to-noise ratio (SNR). Uses four redundant sites
1994	McLaughlin	•		Screenprinted Ag/AgCl (no gel)	
1994	Taheri <i>et al</i>		•	Si_3N_4 on steel	High SNR. Low frequency signal present due to electrode movement
1992	Nishimura <i>et al</i>	•		Stainless steel	
1990	Padmadinata <i>et al</i>	•		Silver, stainless steel	
1989	Geddes and Baker	•	•		Effective dielectric thickness changes with dry skin layer and perspiration
1979	Griffith <i>et al</i>		•	Tantalum pentoxide	Films robust until heavily scratched
1979	De Luca <i>et al</i>	•		Stainless steel	
1974	Ko and Hynecek		•	SiO_2 on Si	Electric field problems. Motion artefact a problem due to long settling time from RC constant
1973	Matsuo <i>et al</i>		•	Barium titanate	Material is piezoelectric
1973	Geddes <i>et al</i>	•		Silver	
1972	David and Portnoy		•	BaTiO_3 , TiO_2 , Ta_2O_5 , SiO_2	Insulated electrode less affected by movement artefact. Some loss of low frequency information
1971	Bergey <i>et al</i>	•	•	Ag, Au, brass, stainless steel, anodized Al	Charge sensitive, Al_2O_3 erratic. Movement artefact least with stainless steel, most with Al_2O_3
1971	Lagow <i>et al</i>	•		Anodized Ta and Al	Careful shielding arrangement required
1970	Potter and Menke	•		Pyre varnish	
1969	Wolfson and Neuman	•		Silicon oxide	
1969	Lopez and Richardson	•		Anodized aluminium	
1968	Richardson <i>et al</i>	•		Anodized aluminium	Movement artefacts
1967	Richardson	•		Anodized aluminium	

2.4.1. Electrode material

Biopotential electrode (wet electrodes) must serve as an interface between the body and the electronics and have the capability of conducting current. Current inside the body is formed by ions in body fluid, and current in the electrode is formed by electrons. Therefore chemical reactions happen at the skin surface to transduce current, ions inside the body change valence and electrons flow into or out of the electrode[32]. The oxidation reactions of ions dominate when current flows from electrode to electrolyte. Reversely, reduction reactions of ions dominate.

Different types of electrodes are used: Ag/AgCl, AgCl, Ag, Au, etc. to provide low noise skin-electrode contact. Ag/AgCl electrodes are most commonly used.

As for pure metal Ag electrodes, electric noise is higher than Ag/AgCl electrodes, and a majority of the electric noise is at low frequencies.

2.4.2. Effect of polarization on the electrode potential

Due to polarization, the net current that flows through the electrode is not 0, so the potential on the electrode changes. The three mechanisms that contribute to the overpotential are ohmic overpotential due to resistance of the electrolyte, concentration overpotential due to concentration change of ions, activation overpotential due to potential barrier height change.

$$V_p = E^0 + V_r + V_c + V_a \quad (1.2)$$

Where V_p is the total potential on the electrode, E^0 is the half-cell potential, which is the potential when no net current flows through the electrode-electrolyte surface, V_r , V_c , V_a are caused by polarization.

Equivalent circuit:

Ag/AgCl electrodes are most commonly used as wet electrodes because they are easy to fabricate in the laboratory and approach perfect non-polarizable electrodes.

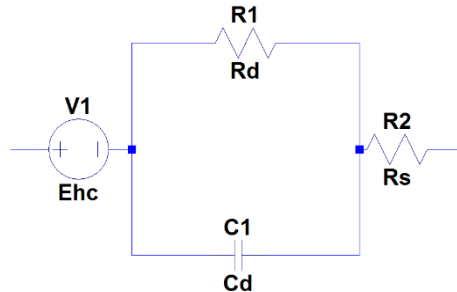


Figure 2.13 Equivalent circuit

An equivalent circuit for wet electrode-skin contact is shown as figure 2.13, R_s is the resistance in the electrolyte of the wet-electrode, and R_d is associated with interface effects. R_d and C_d make up the equivalent impedance (with polarization effects considered) at the electrode-electrolyte interface. E_{hc} is the half-cell potential.

Disadvantages of wet electrodes:

Wet electrodes have some drawbacks. sEMG electrodes used for an application should be suitable for the situation and not influence signal fidelity.

Table 2.2 Disadvantages of wet electrodes and possible solutions

Disadvantages		Possible solutions
powerline interference is limited by electrode/skin contact impedance		active electrodes provide much less emphasis on the skin-electrode impedance
use of an electrolyte is inconvenient	signal quality reduces as the gel dehydrates	Use electrodes without electrolytes like dry electrodes and insulating electrodes.
	reapplication of gel may not be feasible	
	electrodes may be placed in sensitive areas	
	electrodes may be placed so close that electrolyte smears	
	application and removal of the gel is unpleasant	
toxicological concerns with electrolyte gels		

2.5. ADCs

For measuring the EMG signals and conversion to the digital domain, amplifiers and analog-to-digital converters are required. Two suitable, commercially available, amplifier ICs could be the ADS129X family (consisting of a programmable gain amplifier PGA with ADCs included) or the AD8233 (bio amplifier only). They consume a small amount of power and have high CMRR, the small package of the chips provides the possibility to integrate them into a wearable device or sportswear. In table 2.3, the most important parameters of ADS1299 and AD8233 chips are listed.

Table 2.3 Comparison of chips

	ADS1299			AD8233
	ADS1299	ADS1299-4	ADS1299-6	
Channel(s)	8	4	6	1
Resolution (Bits)	24			—
CMRR (dB)	110			80
Sampling rate (Max) (SPS)	250 to 16 k			—
internal processing	$\Delta\Sigma$ ADCs with PGA, internal reference, and an onboard oscillator			Accepts up to ± 300 mV of half-cell potential
Gain	1, 2, 4, 6, 8, 12, 24			100
Power consumption (Typ)	42(mW)	24(mW)	33(mW)	Low quiescent supply current: 50 μ A
Analog power supply (V)	4.75 to 5.25			1.7 to 3.5
Digital power supply (V)	1.8 to 3.6			—
Package size	10.00 mm \times 10.00 mm TQFP-64			2 mm \times 1.7 mm \times 0.5 mm or 0.15 mm

3. System Requirements and Measurement Approach

Firstly, an existing commercially available EMG measurement system, Biosignalsplus, is used to do a preliminary measurement, the Biosignalsplus EMG sensor could achieve lower than 3000 Hz sampling frequency for 8 input channels maximum simultaneously. The preliminary measurement will be an experiment to record sEMG signals from an exercising athlete. The collected sEMG signals will be analyzed to detect muscle fatigue, this preliminary measurement is presented in section 3.1. Based on the results of the preliminary experiment, the requirements for the new system will be derived (section 3.2). Furthermore, the requirements and conditions for the physical experiments will be discussed in section 3.3.

3.1. Experiment with Biosignalsplus

This experiment aims to see how an sEMG system works and how the sEMG signal change while the athlete is doing exercise.

The materials that are used in this experiment are listed below.

- Electrodes
- Input cables
- A Biosignalsplus hub[33]
- A smartphone
- A computer.

The required software is MATLAB and ‘OpenSignals’ APP which is installed on the smartphone. sEMG signals are sensed by the electrodes and transmitted to the Biosignalsplus through input cables, then the filtered and sampled sEMG signals are sent to the smartphone through Bluetooth and saved as a text file, finally, the saved data are analyzed in MATLAB.



Figure 3.1 Biosignalsplus hub and EMG sensor [34]

In this experiment, the sampling rate is set as 1000Hz, which is ideally the lowest sampling rate, because the expected sEMG frequency range is below 500 Hz, according to the Nyquist

sampling theorem, the continuous-time signal, sEMG signal, could be perfectly reconstructed by the samples if the sEMG signal is sampled over 1000 Hz, which is twice the highest frequency component of sEMG signal.

The electrodes are attached on top of a hamstring muscle and the athlete does the single-leg back kick periodically while recording sEMG signals, the frequency is around 1 time per second. The speed of the exercise is not controlled. The exercise and electrode positions are presented in figure 3.2, the blue dots represent the positions for two input electrodes, and the yellow dot represents the position for the reference electrode.



Figure 3.2 Single-leg back kick

The results of the test are presented in figure 3.3, it is the time-domain sEMG signal. Since the common-mode voltage is constant and its value is zero, it could be derived that a high pass filter is applied to the signal.

Each peak corresponds to a period of muscle contractions, which is a single leg back kick in this experiment. While the time domain signal is at the low absolute value, the athlete's hamstring muscle is at rest.

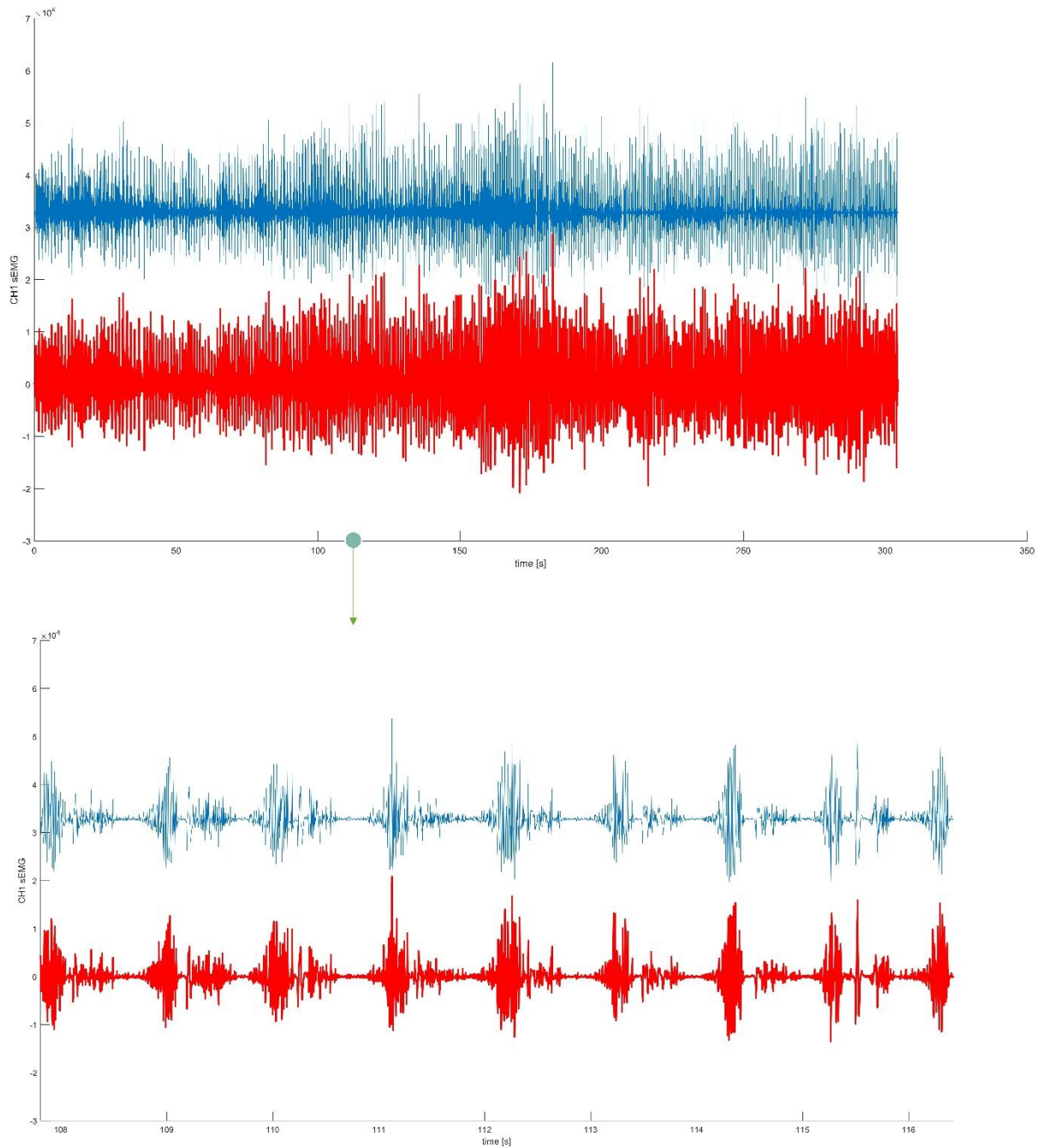


Figure 3.3 Time-domain sEMG signal

It can be seen in figure 3.4 that there is a decrease in MNF from the start time to around 150 seconds. However, MNF increased gradually from around 55 Hz to 70 Hz after that time. Since the athlete did not perform the movement according to a strictly repetitive pattern, the exercise power or speed is not controlled, there exist various possibilities why the decrease and increase occurred. A reason for the increase could be that the athlete produced less power.

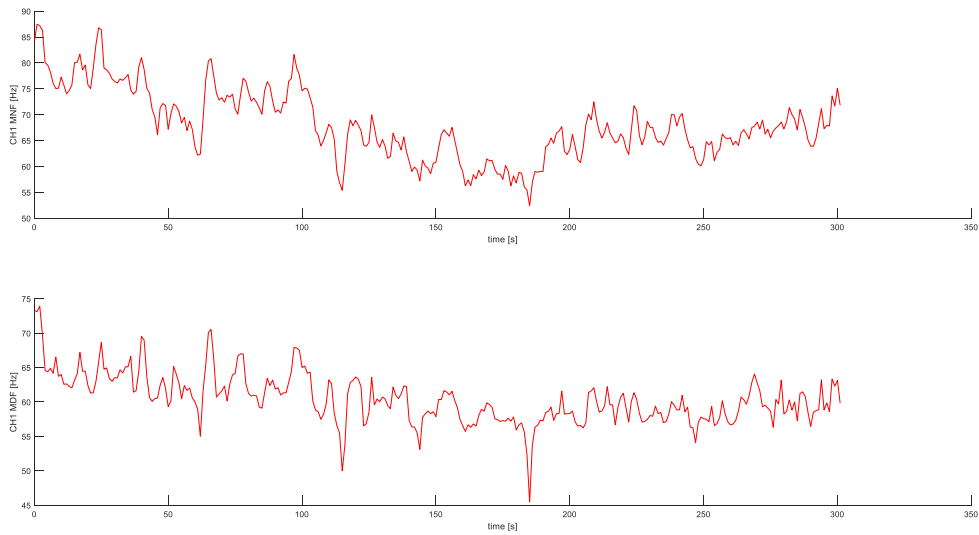


Figure 3.4 sEMG MNF/MDF vs. time

Muscle fiber propagation velocity (MFPV) analysis has also been done on two groups of sEMG signals in this experiment, they are measured on the same muscle with about 2 cm distance. The signals ‘x, y’ are rectified and converted into envelopes ‘rx, ry’, then the ‘finddelay(ry, rx)’ MATLAB function is used to calculate time delay between both signals. However the aim of observing a decrease in MFPV is not achieved, this could be caused by the severe movement artifact noise, low sampling rate and interference from different muscles.

Muscle movements relative to the skin during exercises cause the movement artifact noise. In this experiment, the exercise is not an isometric exercise, so there is a continuous change in muscle length and muscle – skin relative position.

Isometric exercise and isotonic exercise

Isometric exercises and isotonic exercises are commonly used in EMG signal recording experiments. During an exercise, if the muscle length remains the same, it could be described as an isometric exercise. If the muscle length varies but the muscle tension remains the same, the exercise could be described as an isotonic exercise.

The advantage of doing isometric exercises in sEMG recording experiments is that the posture of the athlete is controlled, so there will be less motion artifact noise compared to other exercises that are not stationary. And the advantage of doing isotonic exercises is that the power is controlled, so the muscle performs at a stable workload.

In conclusion, the new system is expected to be able to measure sEMG signals of sufficient quality to perform MNF and MFPV analysis.

3.2. Requirements for the system

There are different requirements for doing MNF and MFPV analysis, this will be discussed specifically in this section.

3.2.1. Requirements for MNF analysis

MNF analysis is based on the power spectrum of the recorded sEMG signals.

3.2.1.1. Sampling rate

The maximum sEMG signal frequency is 500Hz. Based on the Nyquist Sampling Theorem, the sampling rate should exceed 1000 Hz. To avoid possible aliasing, the sampling rate for doing MNF analysis is designed as 4000 Hz or higher.

3.2.1.2. Input channels

For MNF analysis, a single input channel should be enough for analyzing muscle fatigue in one muscle. More channels could record more than one muscle sEMG at the same time, however, this requires higher data transfer speed. In this project only one muscle will be studied at one time, so multiple sEMG signal input channels are unnecessary for doing basic MNF analysis on a single muscle.

3.2.1.3. Exercise type

The sEMG signals are measured from the skin, so there should be inevitable movement artifact noise. The noise could be reduced by doing isometric exercise. For MNF analysis, the exercise types can be both isotonic exercise and isometric exercise. The differences in the results will be discussed.

3.2.2. Requirements for MFPV analysis

The signal of interest in this analysis is the time delay between the sEMG signals recorded from the two pairs of input electrodes placed on the same muscle.

3.2.2.1. Input channels

There should be at least 2 input channels for MFPV analysis. The 2 channels should measure the same muscle, there are 2 input electrodes for each channel, and they are placed along with the direction of muscle fiber to record time delay in the sEMG. The distance between the 2 channels is dependent on the size of the electrodes. The NM 3351 OFI electrodes are used in the experiments, the electrode size is shown in figure 3.5, the dimensions are $51 \times 33 \text{ mm}$.



Figure 3.5 NM 3351 OFI electrode[35]

The electrodes are placed next to each other alongside with the direction of the muscle fiber. If 4 input electrodes are used for 2 input channels, the distance between 2 channels is about 66mm. If only 3 electrodes are used for 2 input channels, which means channel 1 and channel 2 share an input lead, in this condition the distance between 2 input channels is 33mm.

3.2.2.2. Sampling rate

The MFPV ranges from about 3 m/s to 5 m/s and could be reduced by muscle fatigue. The sampling period should be shorter than the time delay between the two recorded sEMG signals. The minimum time delay is about 6.6 ms (5 m/s, 3.3 cm spacing), so the sampling rate should exceed 152Hz for MFPV analysis, a higher sampling rate reduces the calculating error. The sampling rate for doing MFPV analysis is designed as higher than 5000 Hz for calculating time delay with less than 0.2 ms error.

3.2.2.3. Exercise type

To reduce the effect of movement artifact noise, the MFPV analysis is for isometric exercise only.

3.2.2.4. Signal filtering

Signal filtering for sEMG signals has always been a compromise between less noise and more sEMG signal power. Especially MFPV analysis is in favor of less noise. There is a lot of noise in the 0-20 Hz frequency band, so the digital high pass filter for this analysis is designed with a 20 Hz cut-off frequency. There will be some sEMG data loss between 10 to 20 Hz, however, the low-frequency noises present in this range will be canceled. The low pass filter is designed for filtering out white noise above the sEMG frequencies of interest. The low-pass filter, therefore, is designed with a cut-off frequency of around 1000 Hz.

Table 3.1 System Requirements

	MNF analysis	MFPV analysis
Sampling rate	$\geq 4000\text{Hz}$	$\geq 5000\text{Hz}$
The number of the input channel(s)	≥ 1	≥ 2
Exercise type(s)	Isometric or isotonic exercise	Isometric exercise
Input voltage range	30mV	30mV
Input resolution	1 μV	1 μV

3.3. Experimental requirements

As stated in section 3.2, both isometric and isotonic exercises will be done in this experiment. The sign of muscle fatigue could be configured as a failure to maintain the required or expected force[36]. So, both exercises require the athletes to keep the work power uniformly over time until they cannot maintain the designed movement speed in the isotonic exercise or they cannot keep the required posture in the isometric exercise.

3.3.1. The measured muscle

The muscle that gets fatigued in the exercise and has a significant impact on the performance of the athlete will be measured. Such muscles are Biceps brachii, Triceps brachii, Erector spinae, Gluteus, Quadriceps femoris, Biceps femoris, Tibialis anterior, Gastrocnemius, etc. Human muscles and the suggested EMG electrodes positions on the muscles are shown in figure 3.6.

Fine Wire Sites:

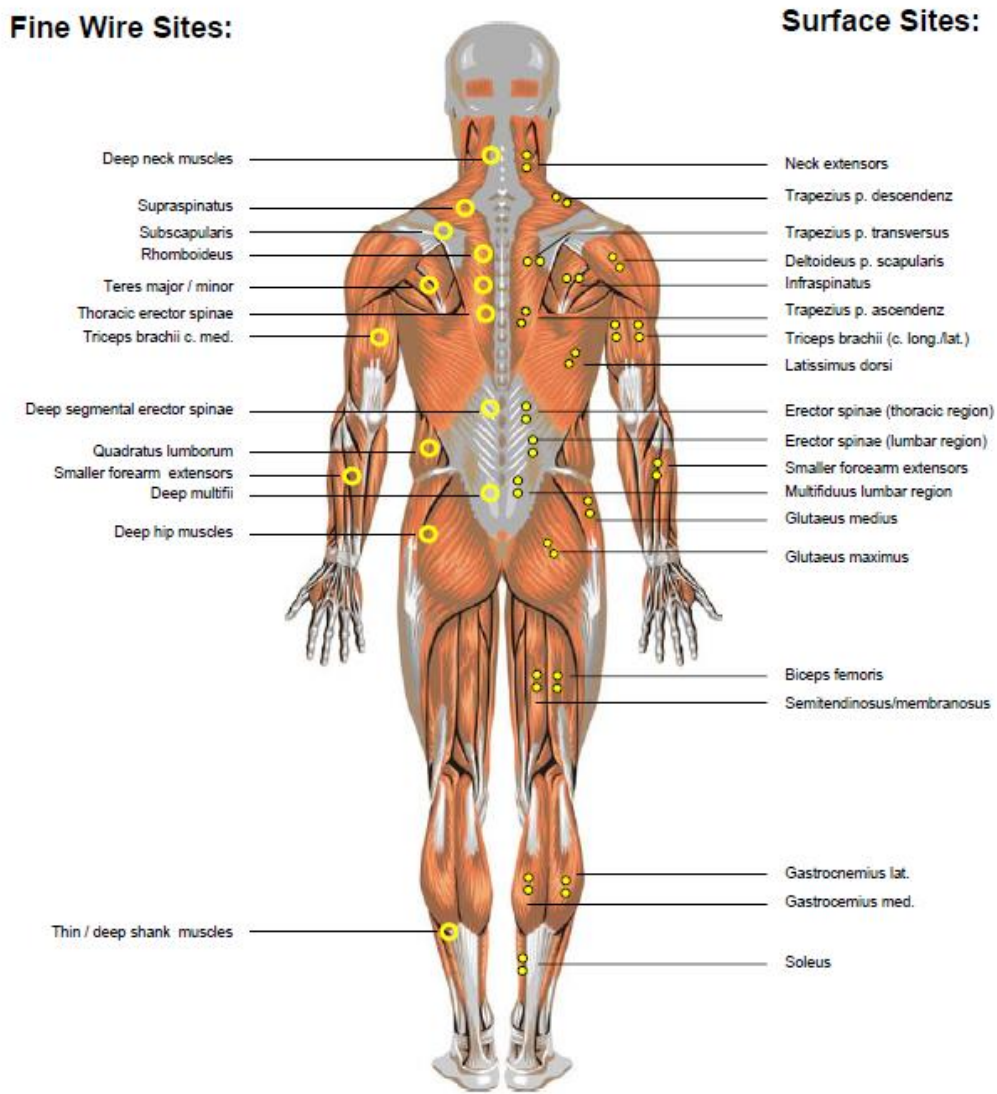
Smaller face muscles
 Smaller neck muscles
 Pectoralis minor
 Diaphragma
 Smaller forearm muscles
 Transversus abd.
 Iliacus
 Psoas major
 Adductors (selective)
 Vastus intermedius
 Thin / deep shank muscles
 Smaller foot muscles

Surface Sites:

Frontalis
 Masseter
 Sternocleidomastoideus
 Deltoides p. acromialis
 Deltoides p. clavicularis
 Pectoralis major
 Biceps brachii
 Serratus anterior
 Rectus abdominis
 Brachioradialis
 Flexor carpi radialis
 Flexor carpi ulnaris
 Obliquus externus abdominis
 Internus / Transversus abd.
 Tensor fascia latae
 Interosseus
 Adductores
 Rectus femoris
 Vastus lateralis
 Vastus medialis
 Peroneus longus
 Tibialis anterior

(a) Frontal view

Dorsal View



(b) Dorsal view
Figure 3.6 (a), (b) Electrode positions for different muscles [37]

This study prefers a muscle that has a larger surface area underneath the skin so that there will be less signal interference from the other nearby muscles, and more electrodes positions for multiple channel inputs on the same muscle. So the studied muscle is decided to be Vastus Medialis. This muscle is a subdivision of Quadriceps femoris on a human thigh, it is measured on the front side of the thigh, thus it is less likely that the electrodes will fall off due to gravity during exercises.

3.3.2. Isometric exercise

3.3.2.1. The reasons for doing wall sit

There are many isometric exercises like wall sit, plank hold, overhead hold, glute bridge, and body hold. This experiment requires an isometric exercise that is easy for the researcher to keep

the athletes in the same posture over time, and not do harm to the athletes if they get fatigued, cannot maintain the posture, and fall. In summary, wall sit is selected as the isometric exercise in this experiment. Figure 3.7 shows an example of a person doing wall-sit.

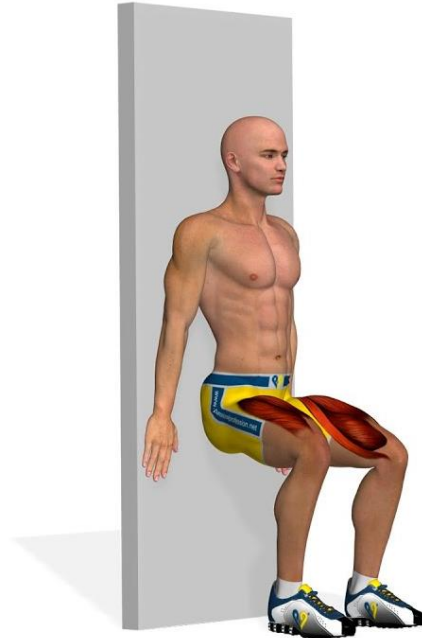


Figure 3.7 Wall-sit [38]

3.3.2.2. The way to record sEMG signals

During wall-sit, the sEMG signals will be measured by multiple input channels, because the recorded signals will be used to do both MNF and MFPV analysis, and MFPV analysis compares the time domain signals from the input channels and calculates time delay, so there should be at least 2 input channels. The input electrodes will be placed along with the direction of the muscle fiber near the midpoint of the muscle. It is shown in figure 3.8. The yellow crosses are the positions for input electrodes, the blue dot is for the reference electrode.

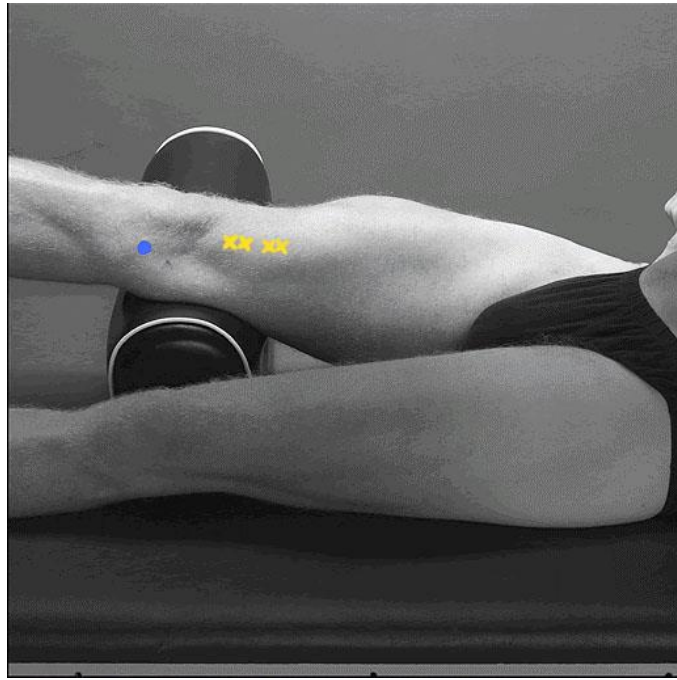


Figure 3.8 positions for electrodes

A tape or an elastic band will be applied on the electrodes in advance to keep the electrodes from falling off.

3.3.2.3. The sign of muscle fatigue

If the athlete gets fatigued in doing wall sit, the athlete's leg will shake and after a while, he or she will slide down. The target time is designed as 100 seconds for beginners and 150 seconds for trained people.

3.3.3. Isotonic exercise

3.3.3.1. The reasons for using a cycling machine

There are a variety of isotonic exercises, for example, jogging, cycling, cross-country skiing, and swimming [39]. In this experiment the required exercise should be easy for the researcher to control its power, also the sEMG measuring device will not be worn on the body, so the athletes should stay at the same place for the experiment.

The cycling machine could be set at a certain speed or power. In this way, the work rate is controlled. To determine the power(resistance level) for each athlete, estimation is performed, the detail is written in the experiment protocol. While doing cycling, the thigh moves near horizontal, this is beneficial for measuring sEMG signals from Vastus Medialis, the reasons have been illustrated in section 3.3.1. In summary, this experiment will use a cycling machine to do isotonic exercises.

3.3.3.2. The way of recording sEMG signals

The sEMG data recorded in this exercise will not be used for MFPV analysis due to the inevitable severe movement artifact noise, so only MNF analysis will be done. To get better sEMG data with less interference from the other muscles and a higher sampling rate, it is recommended that only 1 input channel is used in the experiment.

The input electrodes should be put at the midpoint of Vastus Medialis along with the direction of the muscle fiber, the reference electrode position should refer to the blue dot in figure 3.8.

It is possible that the athletes sweat a lot during this exercise, and this may cause the electrodes to fall off. A tape or an elastic band will be applied on the electrodes in advance to keep them in place.

3.3.3.3. The sign of muscle fatigue

In this isotonic exercise, the athlete is asked to do cycling with a constant speed at 80 rounds per minute (RPM). The power (resistance level) is also constant. The target time is 30 minutes, if the athlete could not keep the cadence as high as 72 RPM, the experiment ends. If the athlete could still cycle after 30 minutes, the experiment will continue until the athlete could not keep the cadence (lower than 72 RPM).

In this chapter, the system requirements and the experiment requirements have been decided based on a preliminary measurement. The summary of system requirements could be found in table 3.1.

4. System Design

The components of this sEMG system are electrodes, input cables, Analog-to-Digital Converters chip with peripheral circuits, microcontroller module with peripheral circuits, and computer. The system structure is shown in figure 4.1.

During sEMG data collection, the electrodes sense the sEMG signals from the athletes, then the signals are transmitted to the ADCs through input cables, the ADCs communicate with the microcontroller using the SPI interface, finally, the microcontroller sends the digital signals to a serial port of the computer.

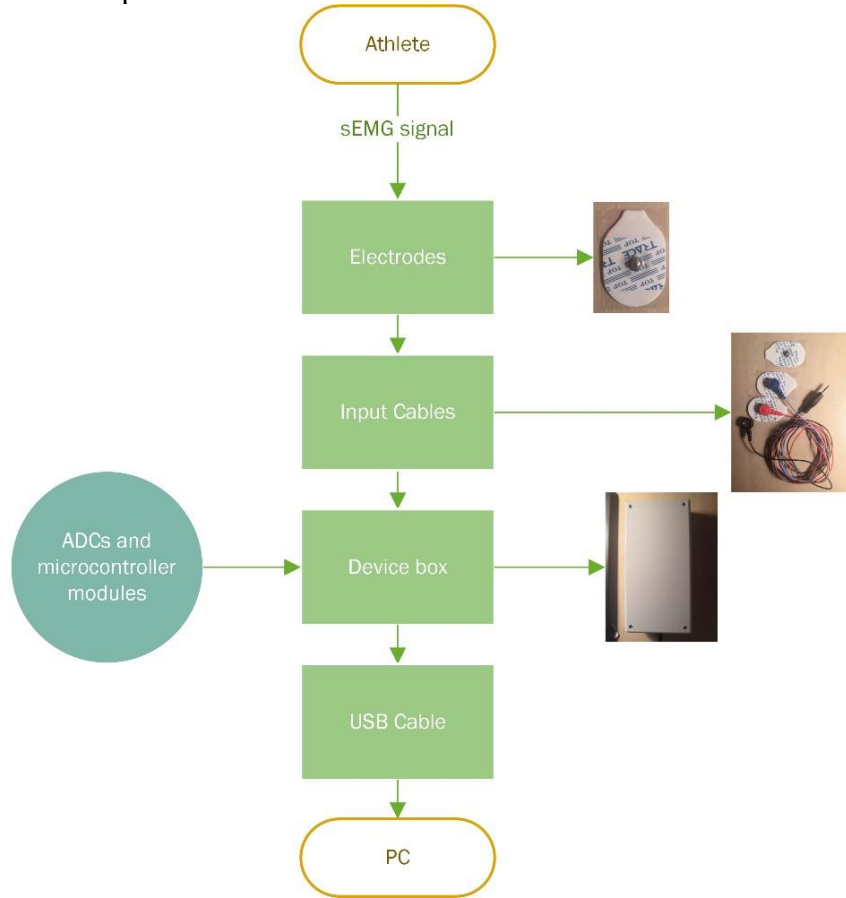


Figure 4.1 sEMG system structure

Figure 4.2 shows the boards and connections inside the device box. The input cables are connected to the ADCs board, the USB cable is connected to the microcontroller board. The SD card and its shield are installed in the box for future use, they are not connected to the microcontroller. A complete circuit diagram of the analog-to-digital converter and a block diagram of the microcontroller could be found in the appendix.

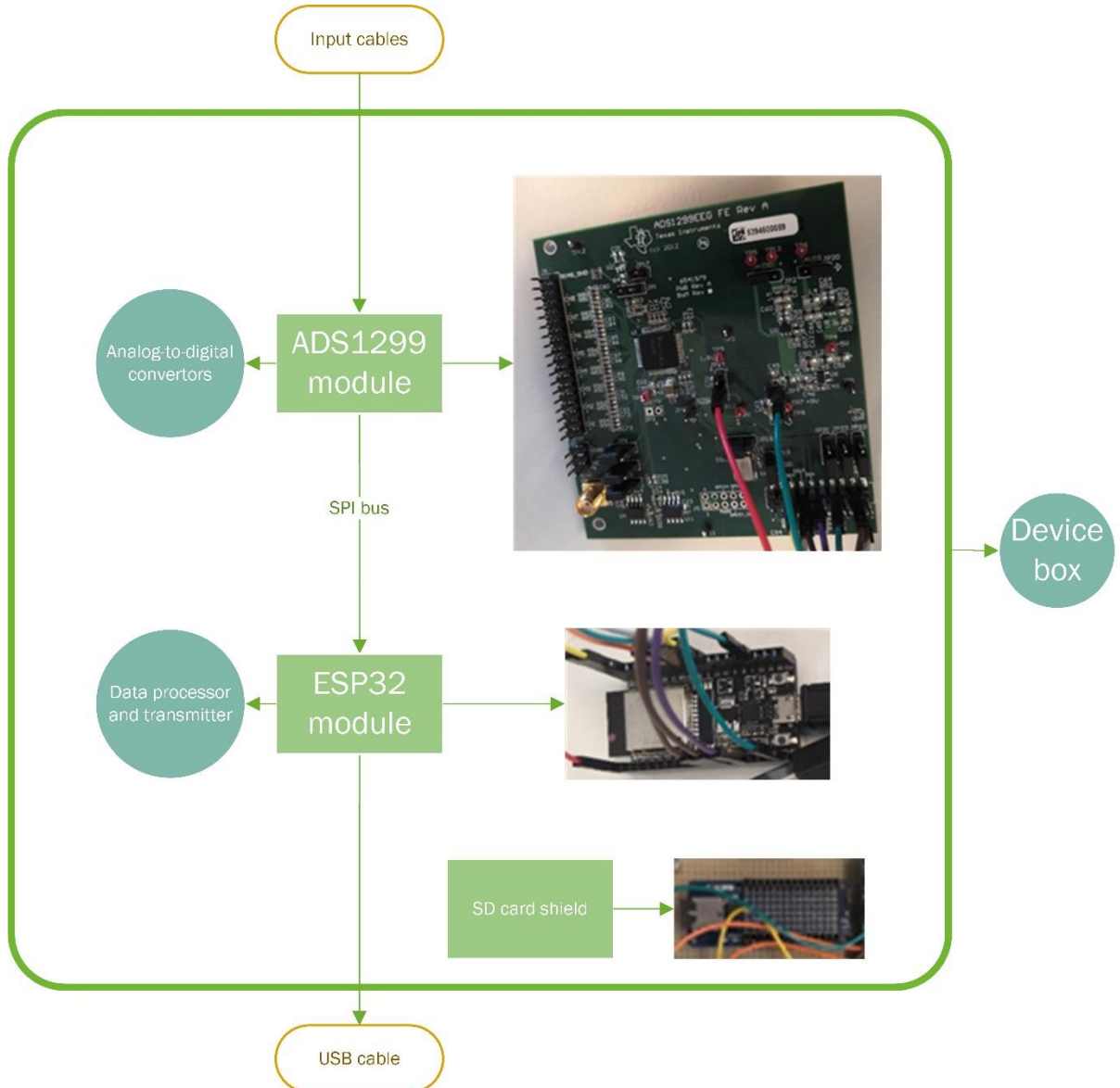


Figure 4.2 sEMG device

4.1. Electrodes and input cables

The electrodes used in this system are Ag/Agcl wet electrodes, NM 3351 OFI. Both electrodes and input cables are commercially available and intended for this purpose.

Figure 4.3 shows two electrodes connected to the differential input pair of a group of input cables. During the experiments, the red wire is configured as the positive input lead, the blue wire is the negative input lead, and the black wire conducts signals from the reference (or bias) electrode.

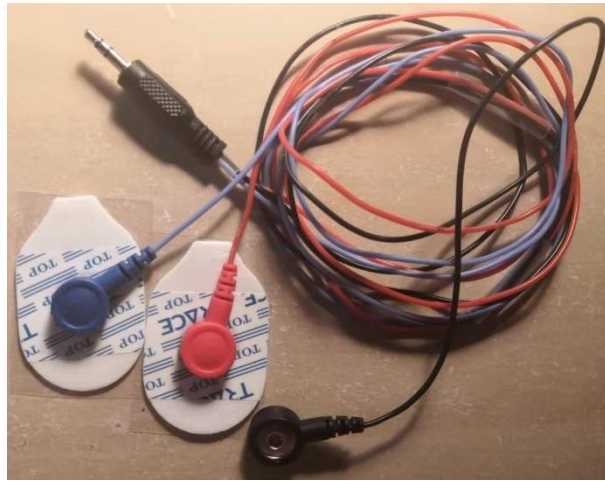


Figure 4.3 Electrodes and input cables

4.2. ADCs

The ADS1299 chip is selected for this sEMG system because of its high ADC resolution (24 bit) and time resolution (sampling rate, SR, could be as high as 16 kSPS), which is suitable for analyzing sEMG signals. Also, it has ADCs integrated with the PGAs (Programmable Gain Amplifier), so it is easier to use than separate amplifiers and ADCs, and its package is suitable for manual soldering. Figure 4.4 is a photo of the ADS1299 board used in this system. The complete circuit diagrams of the ADS1299 chip and the board could be found in the appendix.

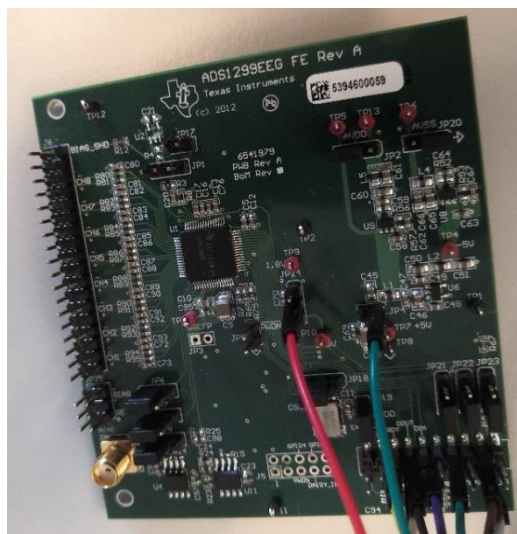


Figure 4.4 ADS1299EEG-FE-Rev-A board

The ADS1299 chip is controlled by the microcontroller through the SPI bus. Figure 4.5 is a flow chart of program design for configuring the ADS1299 chip. The codes could be found in the Appendix.

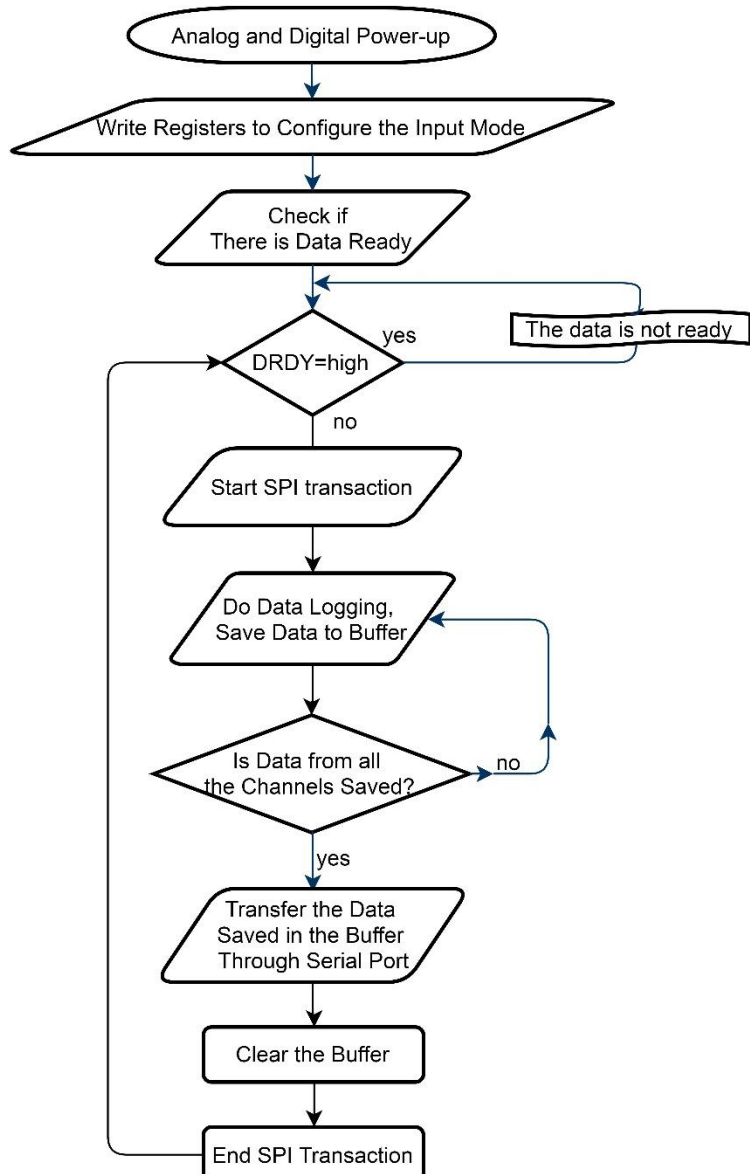
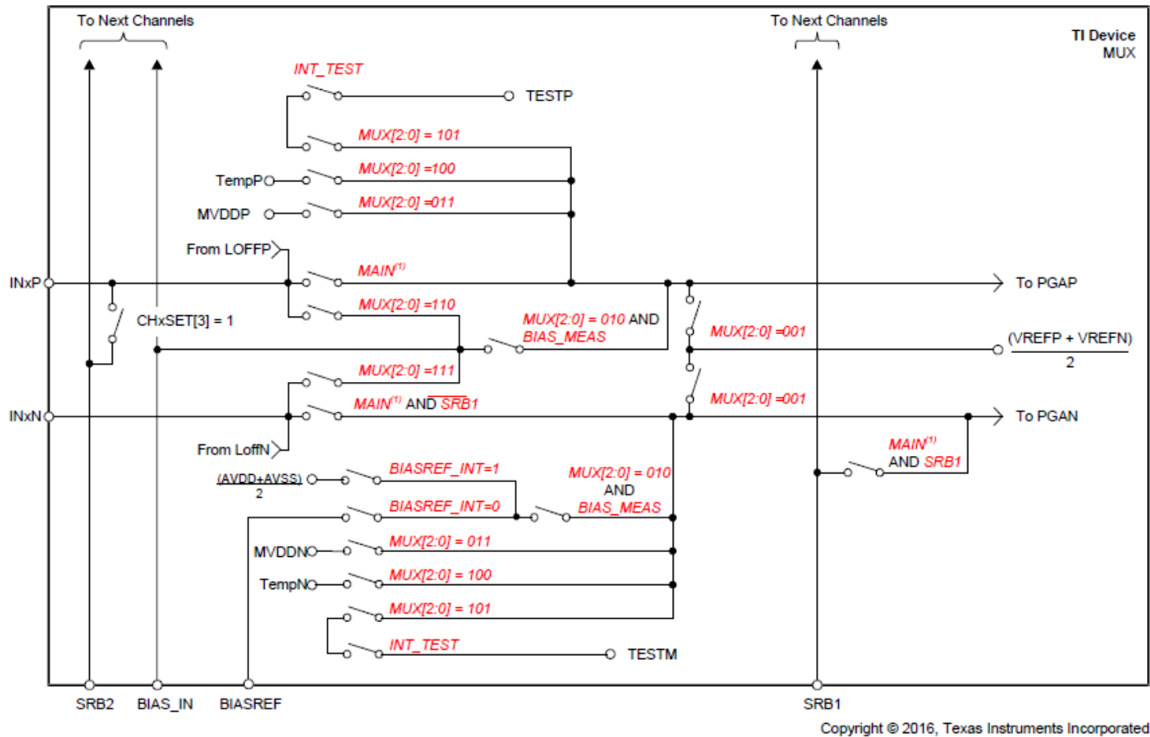


Figure 4.5 Flow chart of ADS1299

The first step is to do the Analog and Digital Power-up, after that the registers are written by commands sent to the SPI.

Figure 4.6 shows the input multiplexer block for channel x (there are 8 channels, $x = 1, 2, 3, 4, 5, 6, 7, 8$). The red words explain MUX values for the corresponding functions like TEST, TEMP, etc. The input modes and descriptions are shown in table 4.2. IN xP and IN xN are the positive input and the negative input of channel x , respectively. The operation mode of the input channel x is controlled by CH x SET register.



Copyright © 2016, Texas Instruments Incorporated

- (1) MAIN is equal to either MUX[2:0] = 000, MUX[2:0] = 110, or MUX[2:0] = 111.

Figure 4.6 Input multiplexer block for one channel[40]

The configuration of registers is listed below in detail.

- Set data rate (DR) by configuring register CONFIG1, in this project the selected data rate is 8 kSPS for 2 input-channel measurements and 16 kSPS(or 8kSPS) for single input-channel measurement. There are some other options for the data rate. The register values of CONFIG1 and their corresponding data rate are shown in table 4.1.

Table 4.1 Register CONFIG1 configuration

Register value	DR (samples/second)
0x90	16k
0x91	8k
0x92	4k
0x93	2k
0x94	1k
0x95	500
0x96	250

- Set test signal generation by configuring register CONFIG2. It can be set to internally generated test signal as well as to an externally generated test signal. The internally generated test signal is a square wave with two options for the frequency. It could help to debug the devices.
- Set reference mode by configuring register CONFIG3, the reference mode is set as the internal reference. The bias signal is generated internally. The bias signal could be generated with a bias measurement loop as well, the voltage on the human body

is measured through an electrode and fed to the bias amplifier, however, this setting occupies an electrode, and the internally generated bias signal fulfills the need of biasing the common-mode voltage, so the bias measurement circuit is not used.

- d. Set the input mode of each input channel by configuring registers CH1SET, CH2SET, CH3SET, CH4SET, CH5SET, CH6SET, CH7SET, CH8SET. During the experiment, only channel 1 and channel 2 are powered up and set in normal input mode. There are many other options for configuring the input channels. The input modes are listed in table 4.2.

Table 4.2 Input channels configuration

Input mode	Description
INPUT NORMAL	Normal electrode input
INPUT SHORTED	Input shorted (for offset or noise measurements)
INPUT MEAS BIAS	Used in conjunction with BIAS_MEAS bit for BIAS measurements
INPUT SUPPLY	MVDD for supply measurement
INPUT TEMP	Temperature sensor
INPUT TESTSIGNAL	Test signal
INPUT SET BIASP	BIAS_DRP (positive electrode is the driver)
INPUT SET BIASN	BIAS_DRN (negative electrode is the driver)

After all the settings are configured, the system checks continuously if the data from the ADCs is ready for transfer. The low level of the DRDY pin indicates that there is a sample from each active input channel ready. All the input channels are sampled simultaneously.

Since each number contains 24 bit, and there could be more than one number transferred in one time because of multiple channels, the transferred data are first saved in a Buffer. When the data transferring from SPI is finished, all the data saved in the Buffer are delivered to the serial port, then the Buffer is cleared, and the system waits for the next group of samples. In this way, the sEMG signals are transferred to the computer continuously.

4.3. Microcontroller

The microcontroller used in this system is ESP32. The reason for using this microcontroller is that it is integrated with Bluetooth, wifi, and it has two SPI buses. So it is capable of controlling multiple sensors at the same time and using different ways to transmit data. Using this microcontroller is beneficial for future extensions of this project. Figure 4.7 is a picture of the ESP32_DevKitc_V4 board. The block diagram of this chip is shown in the appendix.



Figure 4.7 ESP32_DevKitc_V4 board

The firmware run on the ESP32_DevKitc_V4 board is edited and compiled in Arduino-ide and uploaded to the board through a serial port.

The serial port also transmits collected sEMG data from the devices to the computer.

4.4. Computer

The computer works as a firmware and software edit device, data storage device, and data processing and analyzing device in this project.

4.4.1. Data collection

When the digital signals are generated by the ADCs, they are transmitted by the microcontroller to the computer through a serial port immediately. The data is already converted from binary code to decimal numbers, they are saved as '.csv' files. The software that is used to record the data from the serial port is Processing. The data logging codes could be found in the Appendix. A simple flow chart of the data logging procedure is shown in figure 4.8.

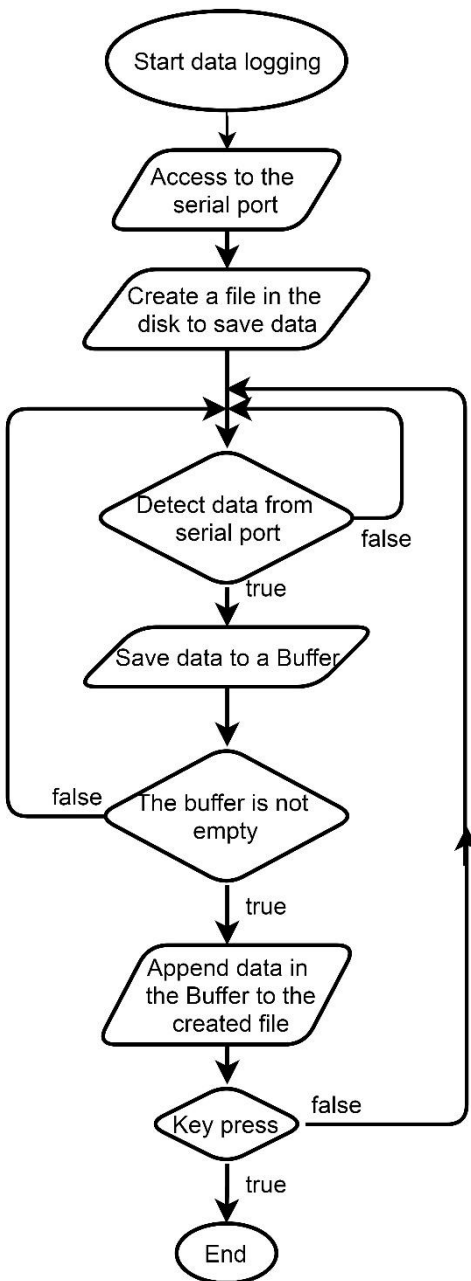


Figure 4.8 Data logging flow chart

4.4.2. Data processing and analysis

Data processing and analysis are done with MATLAB because it is easy to handle complex matrices with MATLAB and a lot of its built-in functions are available for processing and analyzing sEMG data.

4.4.2.1. Data processing

- 1) Repairing data overflow of the ADC

The common-mode voltage of the sEMG signal could be around the ‘0’ or ‘1’ of the ADC, which are the lowest and the highest value of the full scale. So it is necessary to detect data overflow of the ADC in the samples and repair the data.

The way to detect data overflow is to calculate the difference between every pair of two consecutive samples. If the difference is higher than half of the full scale, it could be derived that there exists data overflow. The data overflow is fixed by moving the overflowed series of samples to a full scale higher or a full scale lower. The complete MATLAB code can be found in the appendix.

2) Removing the offset of the recorded signals

Because sEMG signals should have a mean value of zero, the offset of the recorded signals will be removed. This could be achieved by a high pass digital filter with a positive cut-off frequency.

3) Filtering out noises.

The digital filters that are used in this project is a band-pass Butterworth filter and a notch filter. The lower cut-off frequency of the band-pass filter is set as 10-20Hz, the higher cut-off frequency is 500-1000Hz. The notch filter frequency is 50 Hz. After filtering, the time domain waveform should appear to be a series of typical sEMG signals for the isotonic exercise, the resting state, and the contraction duration should be clear to see.

4.4.2.2. Data analyzing

1) Calculating MNF and MDF of the filtered sEMG signals.

MNF/MDF is analyzed within every 3 seconds of sEMG data, the step is set as 1 second. The MNF/MDF is calculated from the start time to the end, and a plot of MNF/MDF versus time is derived. If there is muscle fatigue in the detected muscle, MNF/MDF is expected to shift towards lower value.

2) Calculating MFPV for isometric exercise.

In this project, MFPV could only be analyzed with the sEMG signals measured during isometric exercise. Two channels of sEMG signals are recorded, both channels measured the same muscle. MFPV is related to time-delay between two channels, the distance between 2 channels is about 70mm (Section 3.2.2.1, figure 3.5 shows the size of the electrodes). The time-delay is calculated by MATLAB function ‘xcorr’, then the normalized MFPV vs. time could be derived. The MATLAB code for signal analysis could be found in the Appendix.

The variation of MFPV should be correlated to the change of MNF. When MNF decreases, MFPV is expected to decrease as well.

5. Experiment and Results

It is essential to validate the performance of the sEMG system after the hardware and software design is finished. A physiological experiment is designed and performed for this purpose. This chapter presents the experimental procedure and experimental results. The experiment consists of two parts, the isometric exercise, and the isotonic exercise.

5.1. The experimental procedure

7 athletes have participated in this experiment, all of them are male, around 25 years old, and without the cardiac or muscular disease. Athletes 1-5 have done the isometric exercise, wall-sit, athletes 6-7 have done the isotonic exercise, cycling in the gym. The complete experiment protocol could be found in the appendix.

5.1.1.1. The isometric exercise

Figure 5.1 is a picture of an athlete doing wall-sit. It could be seen in the picture that the floor is slippery, this influenced the wall-sit experiment, some athletes had to adjust position during the experiment because of the slippery floor.



Figure 5.1 Athlete 3 doing wall-sit (Athlete 3)

Figure 5.2 is a picture of electrode positions for the wall-sit experiment. There are 2 groups of input electrodes (red and blue wires) placed on vastus medialis muscle and a reference electrode (black wire) at the knee, the hair was removed and the skin was cleaned before attaching electrodes.



Figure 5.2 Electrode positions for isometric exercise (Athlete 1)

The sEMG system was configured as 2 channel input, 8000 samples per second for both channels. The athlete was first asked to do a thigh muscle contraction to test the connection. When the sEMG waveform could be seen on the laptop, the connection is good, and the experimenter helped the athlete to find the correct feet positions to do wall-sit, then the isometric experiment was ready to start. The athletes tried to do wall-sit as long as possible and tried not to move during the exercise.

5.1.1.2. The isotonic exercise

This experiment is a cycling test. Estimation is performed for the athlete to determine the power (resistance level set up on the cycling machine) during the experiment. First, the experimenter set the resistance level to 10-13, this is determined by the athlete, then the athlete keeps cycling at 80 RPM. The resistance level is increased every 30 seconds until the athlete could not cycle at 80 RPM for 30 seconds. The resistance level during the measurement is 2 levels lower than the last resistance level in estimation.

After the estimation, the athlete should rest for 15 minutes. In the meantime, the experimenter could help the athlete to do skin preparation and place the electrodes.

Figure 5.3 is a picture of electrodes and tapes applied to an athlete for the isotonic exercise. Because people sweat a lot in this experiment, tapes are necessary for keeping the electrodes in place. The tapes are elastic and do not hinder the athletes when they are doing exercise.



Figure 5.3 electrodes and tapes for isotonic exercise (Athlete 6)

The skin preparation is the same as for the isometric exercise. To avoid short circuits between electrodes, a small amount of Vaseline is applied to the skin between the electrodes. After the connection test, the sEMG system started to record sEMG signals, and the athlete was asked to cycle at 80 RPM until he could not keep the cadence (i.e. it drops below 72 RPM).

5.2. The experimental results

5.2.1. Wall-sit

In this section, the results of the mean frequency power spectrum (MNF) and the median frequency power spectrum (MDF) analysis and muscle fiber propagation velocity (MFPV) are presented. The sEMG signals are collected from thigh muscle of 5 athletes doing wall-sit.

5.2.1.1. Wall-sit for 70 seconds (Athlete 1)

In this experiment, the athlete did not move a lot, however, the muscle started to tremble at around 30 seconds. The decrease in MNF and MDF is clear to see in figures 5.4 and 5.5. The blue lines are MNF and MDF calculated in every 3 seconds of sEMG signals, the red lines are polynomial fit of blue lines. The degree is 4. The orange lines are moving mean of blue lines. This athlete does not usually do physical exercise.

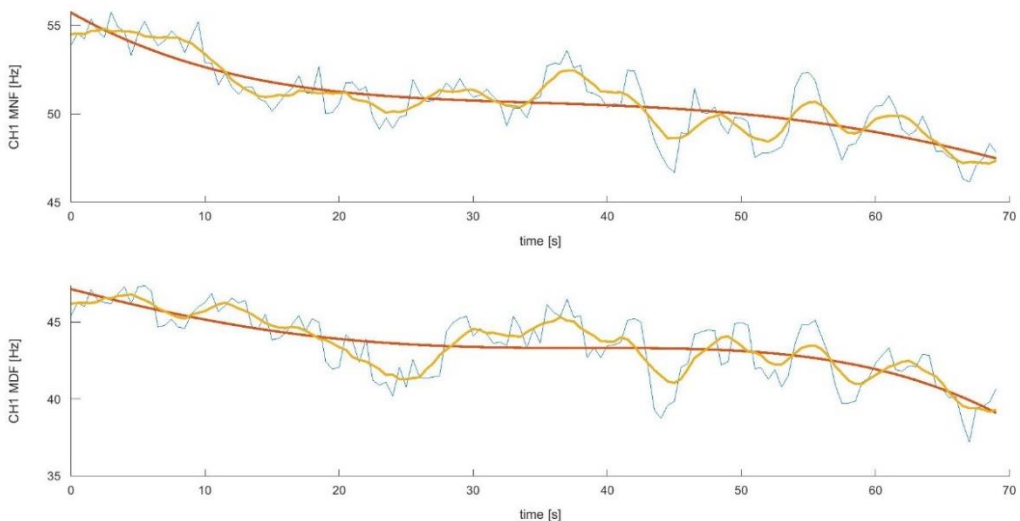


Figure 5.4 Channel1 MNF & MDF, Athlete1

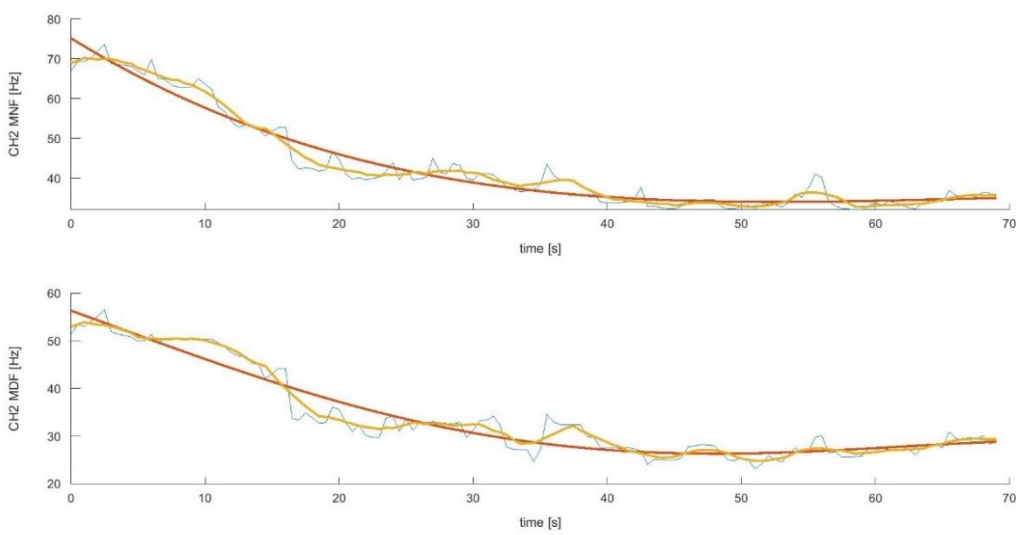


Figure 5.5 Channel2 MNF & MDF, Athlete1

Figure 5.6 shows the normalized MFPV change during this experiment. The trend of MFPV is similar to MNF and MDF of channel 2.

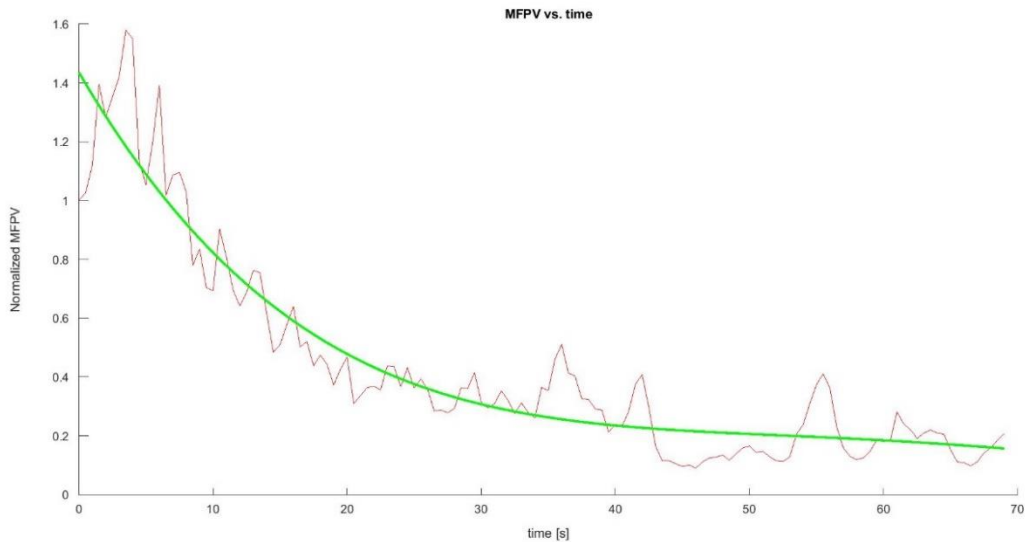


Figure 5.6 MFPV, Athlete 1

5.2.1.2. Wall-sit for 65 seconds (Athlete 2)

This athlete moved and adjusted position during the experiment, a few fluctuations in the MNF and MDF curves in figures 5.7 and 5.8 could be seen. This athlete does not usually do physical exercise.

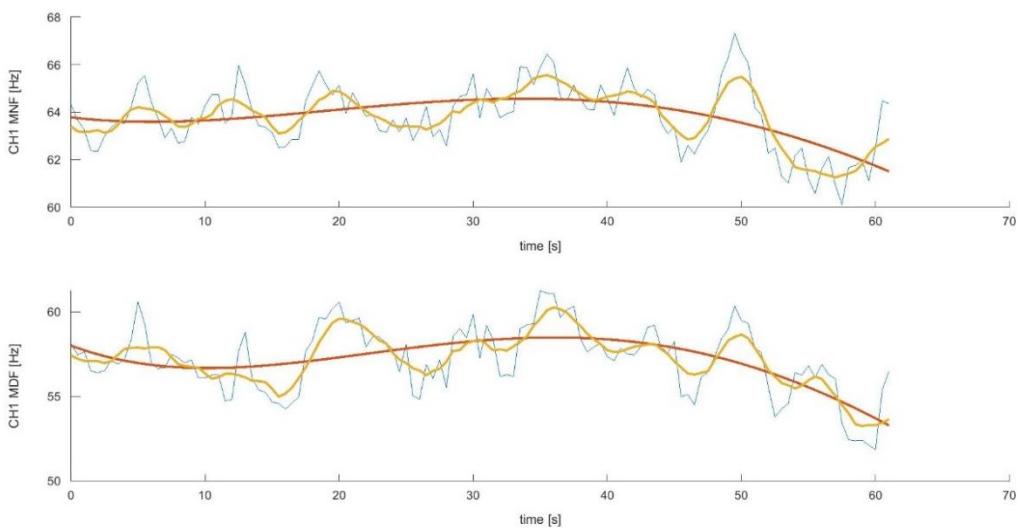


Figure 5.7 Channel1 MNF & MDF, Athlete2

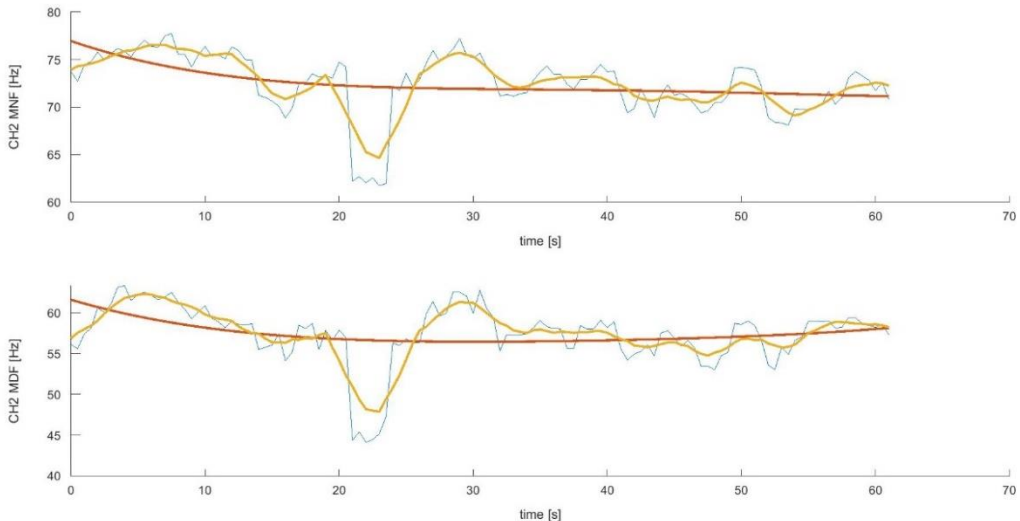


Figure 5.8 Channel2 MNF & MDF, Athlete2

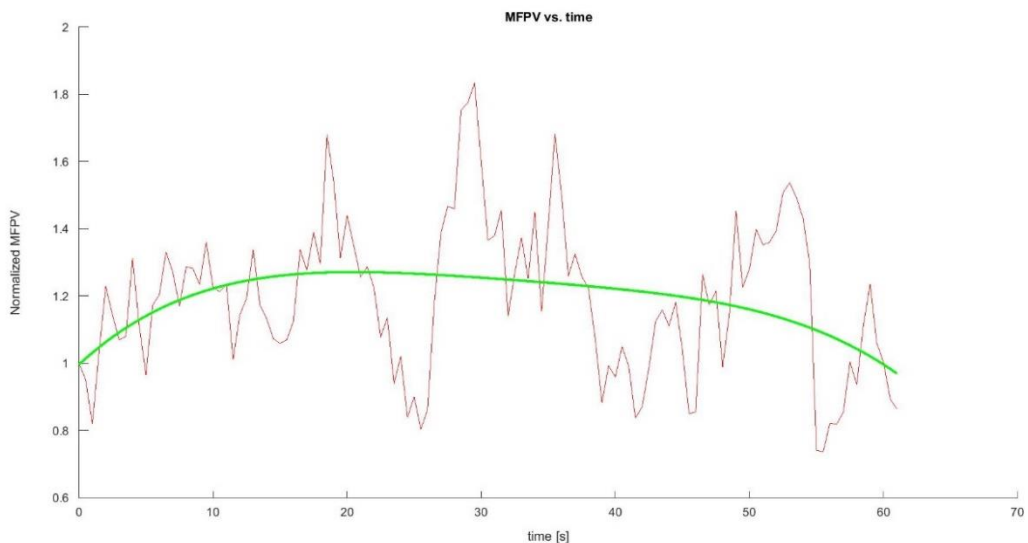


Figure 5.9 MFPV, Athlete 2

5.2.1.3. Wall-sit for 2 min (Athlete 3)

This athlete does physical exercise often, during this experiment he moved for 1 or 2 times to prevent position change, and there are 2 severe fluctuations in figure 5.11. Compared to athlete 2, the signals from channel 1 and channel 2 are more similar for this athlete. This is because athlete 3 does exercise often, he has stronger muscle than athlete 2. So the surface area of muscle is bigger, and both channels have recorded stronger sEMG signals from the muscle.

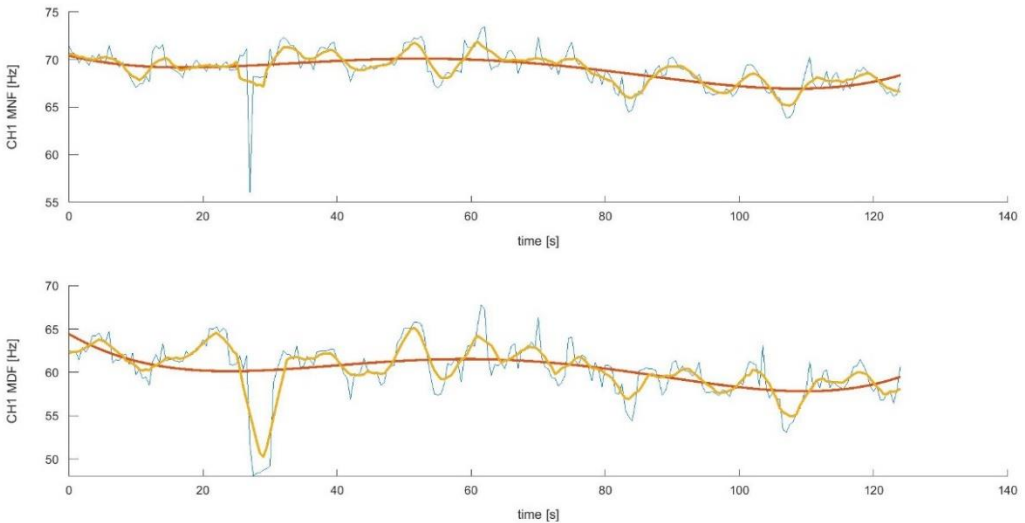


Figure 5.10 Channel1 MNF & MDF, Athlete 3

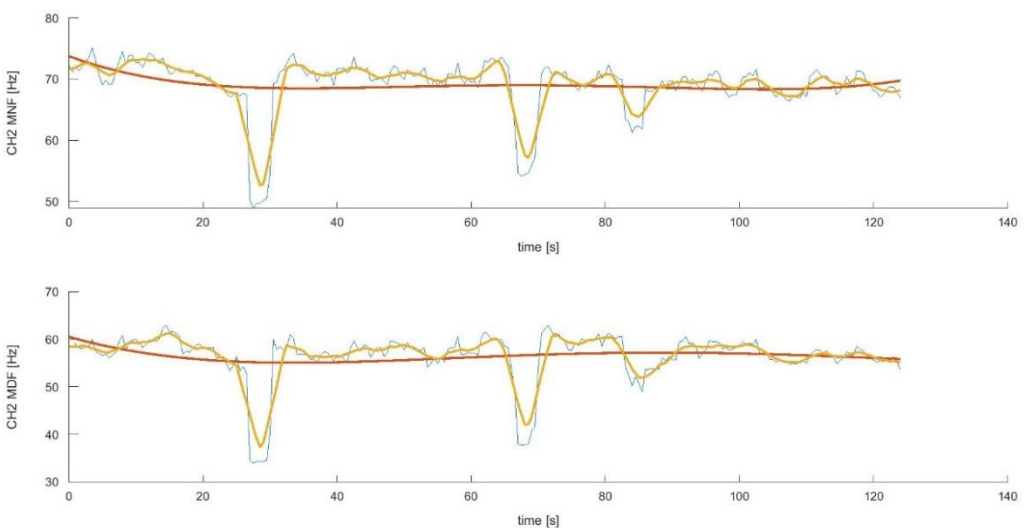


Figure 5.11 Channel2 MNF & MDF, Athlete 3

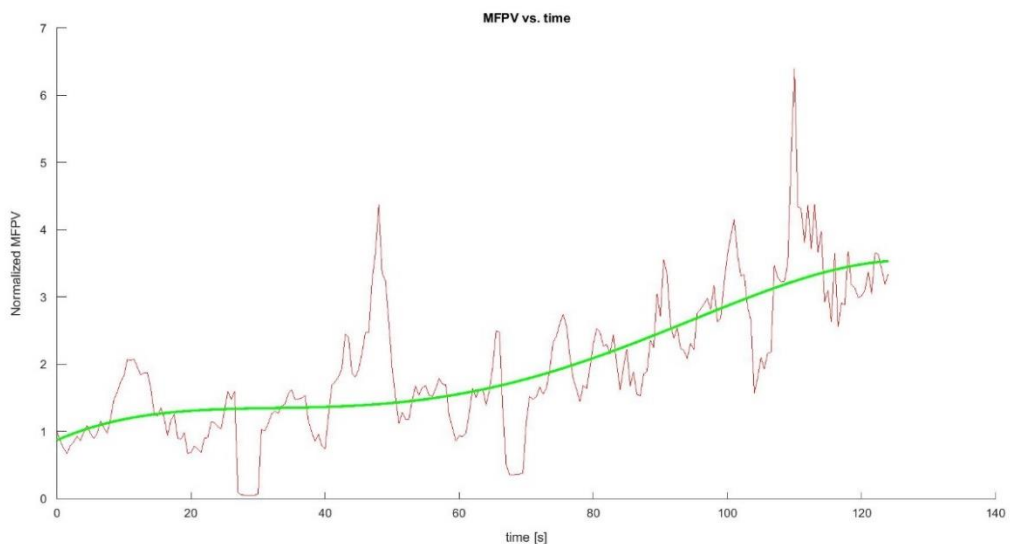


Figure 5.12 MFPV, Athlete 3

5.2.1.4. Wall sit for 2.5 min (Athlete 4)

This athlete does physical exercise often. This athlete also adjusted position during the experiment, a few fluctuations due to the movements could be seen in figures 5.13 and 5.14.

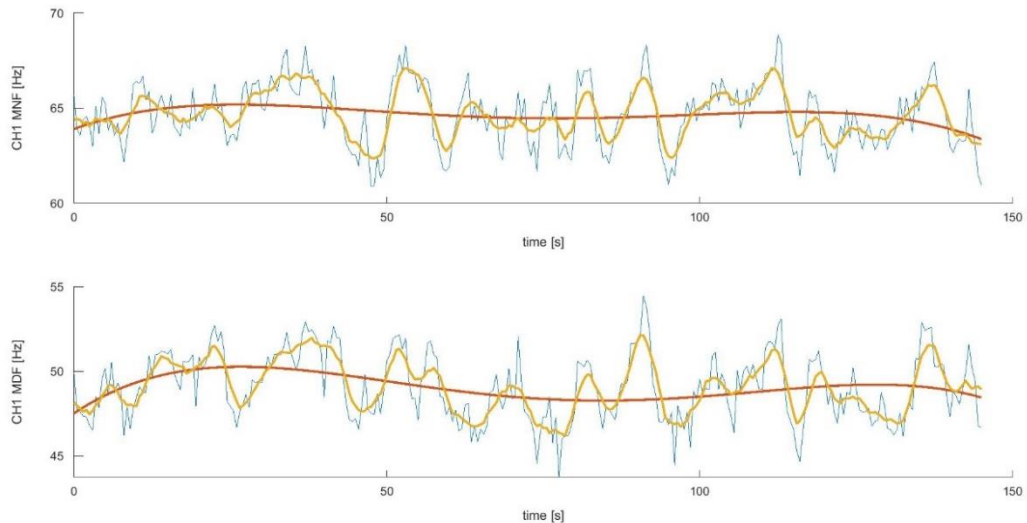


Figure 5.13 Channel 1 MNF & MDF, Athlete 4

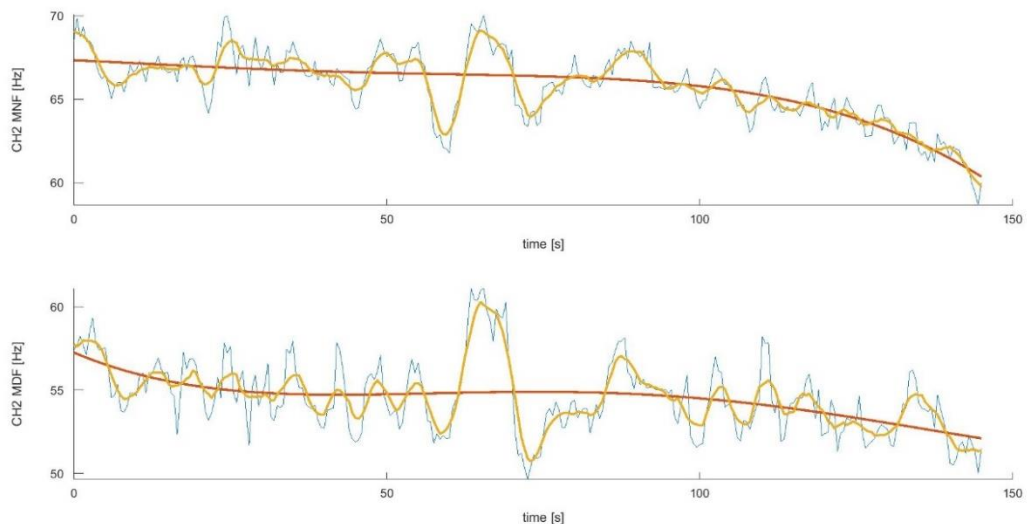


Figure 5.14 Channel 2 MNF & MDF, Athlete 4

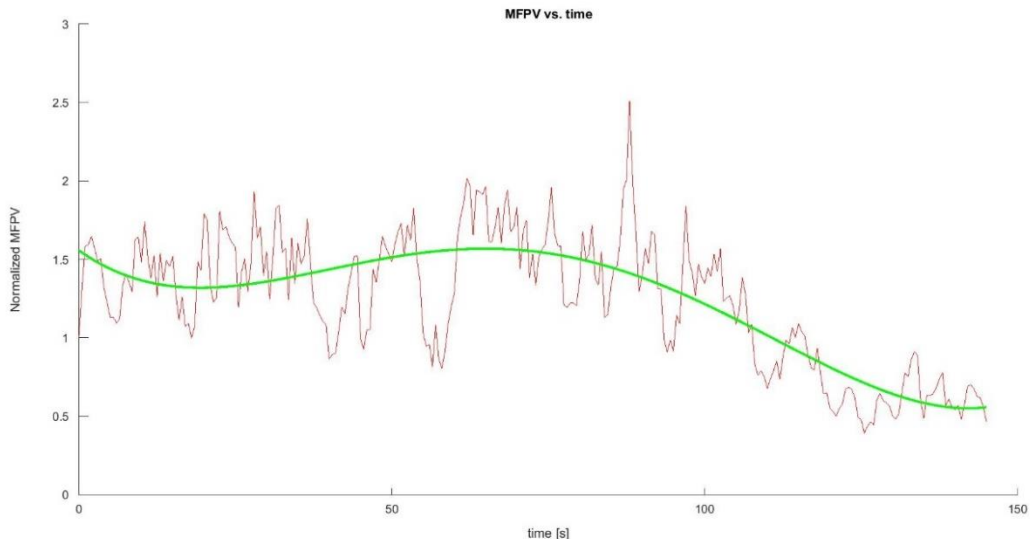


Figure 5.15 MFPV, Athlete 4

5.2.1.5. Wall-sit for 185 seconds and 130 seconds (Athlete 5)

This experiment is done at a different place from the other wall-sit experiment, the noise of 50 Hz AC main is more severe. This athlete does physical exercise often. The athlete first did 185 seconds wall-sit, and rested for over 30 min, after that he did wall-sit again for 130 seconds. Figures 5.16, 5.17, 5.18 are the data analysis results of the first wall-sit experiment, there is a decrease in MNF and MDF for both channels, and the waveforms in figures 5.16, 5.17 have similar shapes.

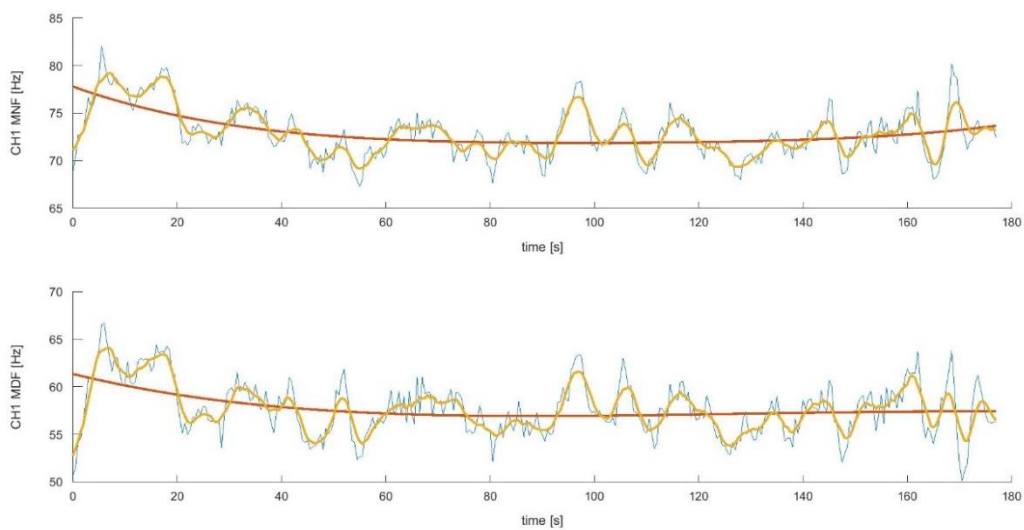


Figure 5.16 Channel 1 MNF & MDF, Athlete 5, Wall-sit 1

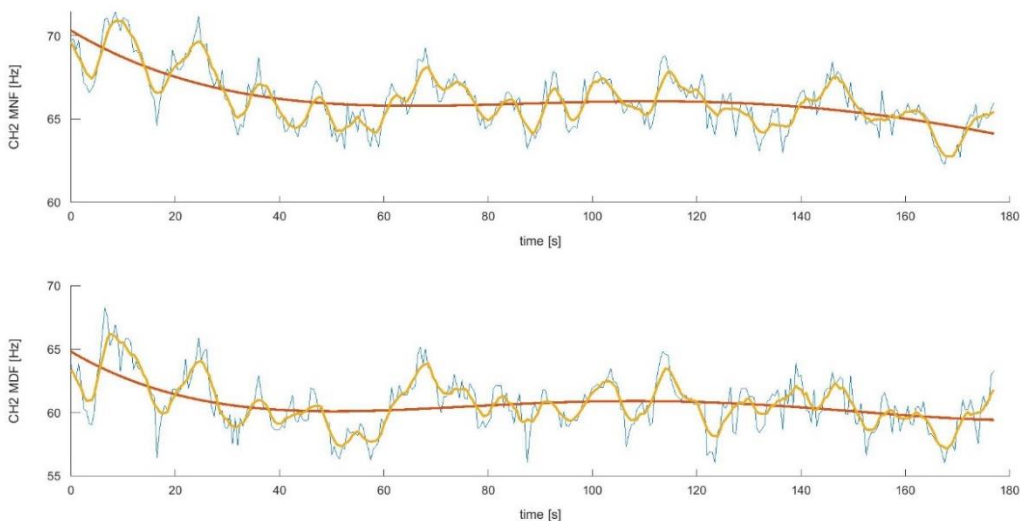


Figure 5.17 Channel 2 MNF & MDF, Athlete 5, Wall-sit 1

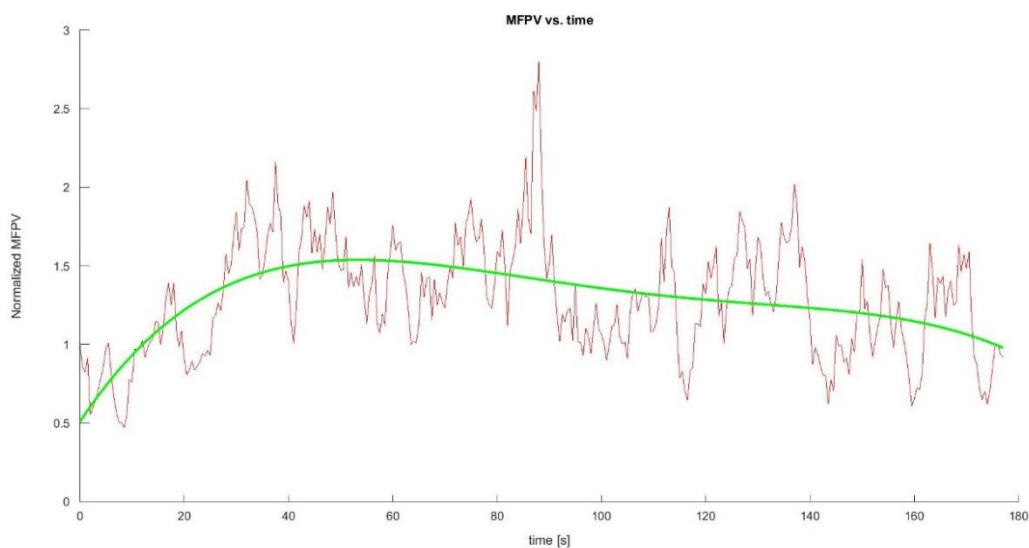


Figure 5.18 MFPV, Athlete 5, Wall-sit 1

Figures 5.19, 5.20 are MNF and MDF analysis of the second wall-sit experiment. Compared to the first experiment of this athlete, the maximum MNF and MDF are about 4 Hz higher, and the exercise time is shorter.

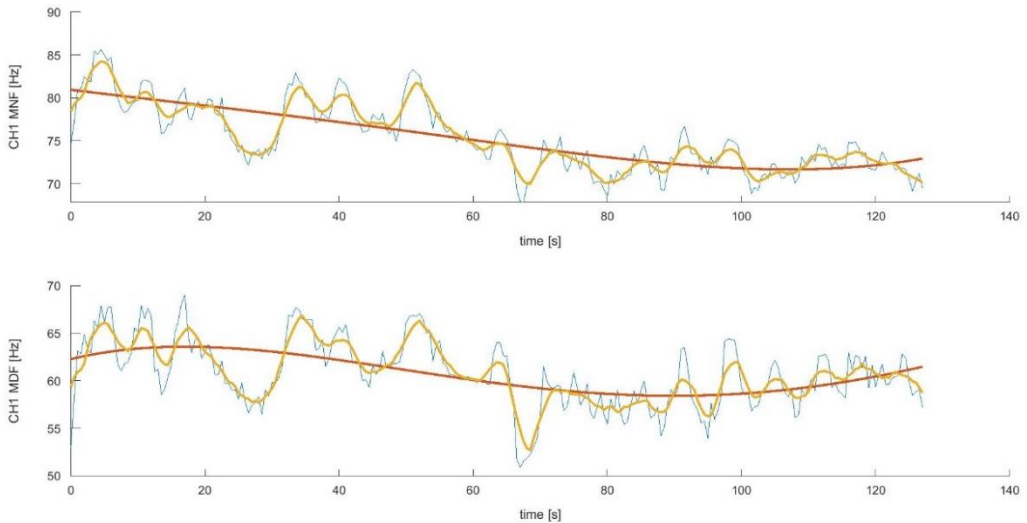


Figure 5.19 Channel 1 MNF & MDF, Athlete 5, Wall-sit 2

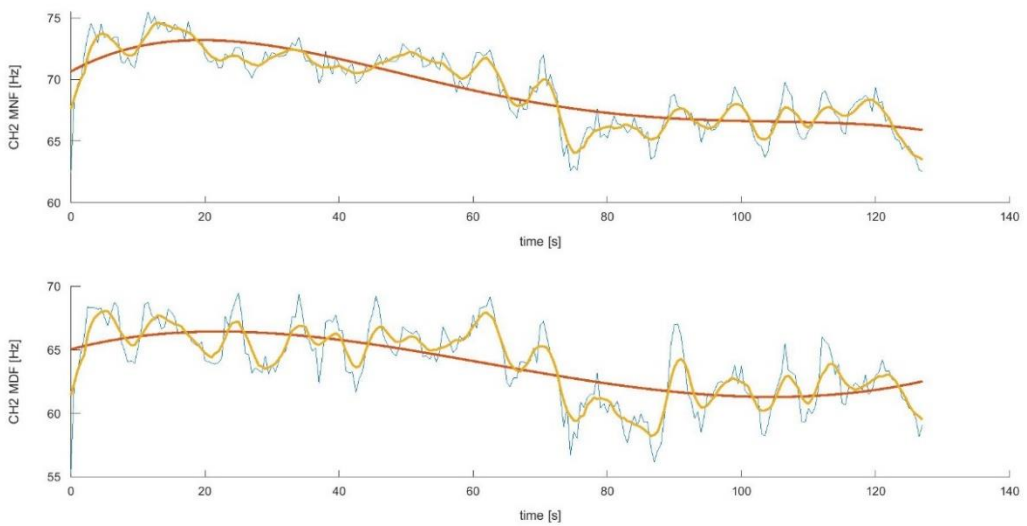


Figure 5.20 Channel 2 MNF & MDF, Athlete 5, Wall-sit 2

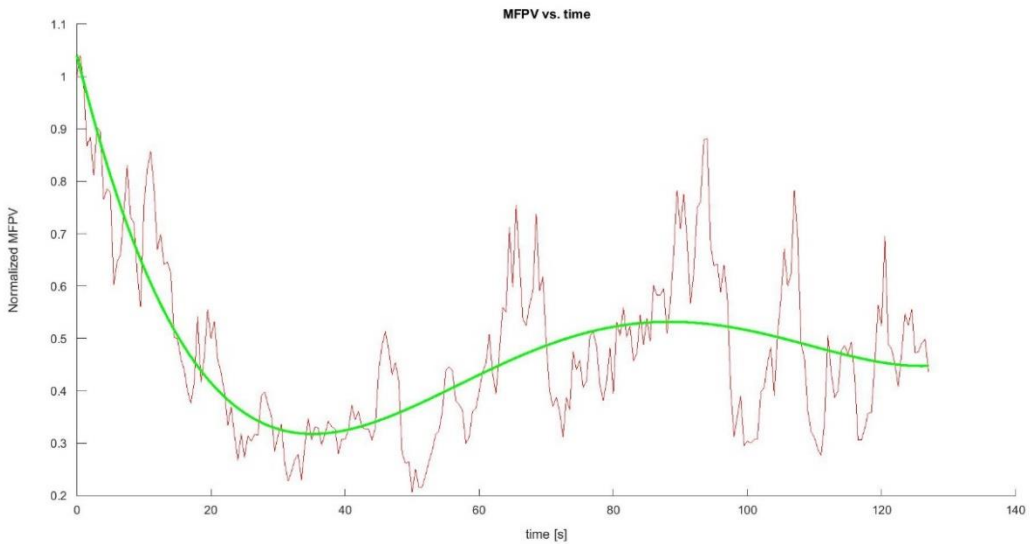


Figure 5.21 MFPV, Athlete 5, Wall-sit 2

5.2.1.6. Wall-sit conclusion

In summary, there is a decrease in MNF and MDF during the wall-sit experiment, MDF is relatively lower than MNF, the waveform of channel 1 and channel 2 usually have a similar trend. And the results for fit and unfit athletes are different. For the unfit athlete, MNF and MDF decrease quickly after the beginning of the experiment.

5.2.2. Isotonic exercise, cycling

In this section, the results of MNF and MDF analysis are presented. The sEMG signals are collected from thigh muscle of 2 athletes during cycling. There is 1 input channel. The MATLAB code for signal analysis could be found in the Appendix.

5.2.2.1. 35 min cycling (Athlete 6)

This athlete does physical exercise often, the exercise types include cycling and running. The resistance level (16) and speed (80 RPM) are constant. Figure 5.22 shows the raw sEMG and filtered sEMG signals during the experiment, there is a band-pass filter (20-500 Hz) and a notch filter (50Hz), the common-mode value is removed by a high pass filter, so the red line in figure 5.22 is near 0.

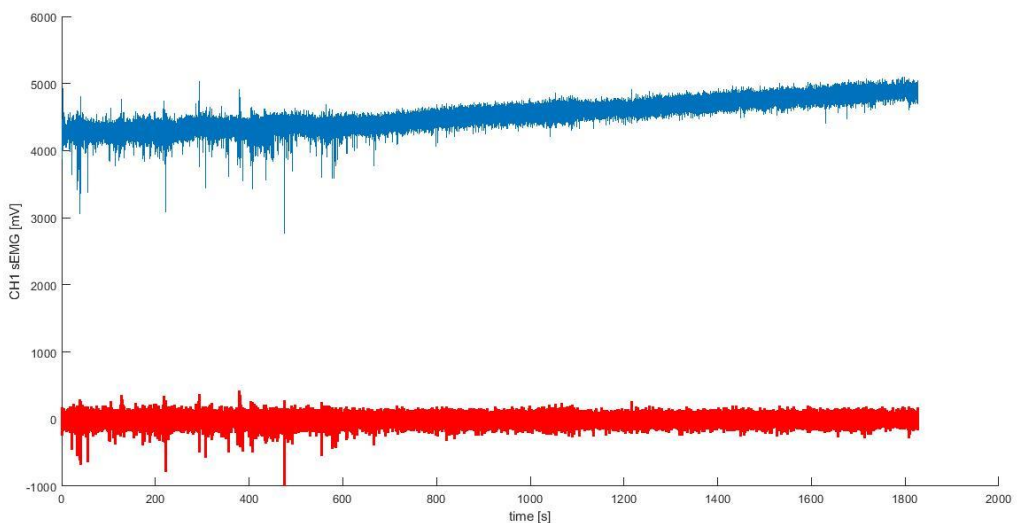


Figure 5.22 raw sEMG (blue) and filtered sEMG (red)

Figure 5.23 (a) is the raw sEMG signal, figure 5.23 (b) is the filtered sEMG signal. Two filters have been applied, a band-pass filter (20-500 Hz) and a notch filter (50 Hz).

Figure 5.23 (c) is the periodogram frequency spectrum analysis of raw sEMG signal, figure 5.23 (d) is the periodogram frequency spectrum analysis of filtered sEMG signal.

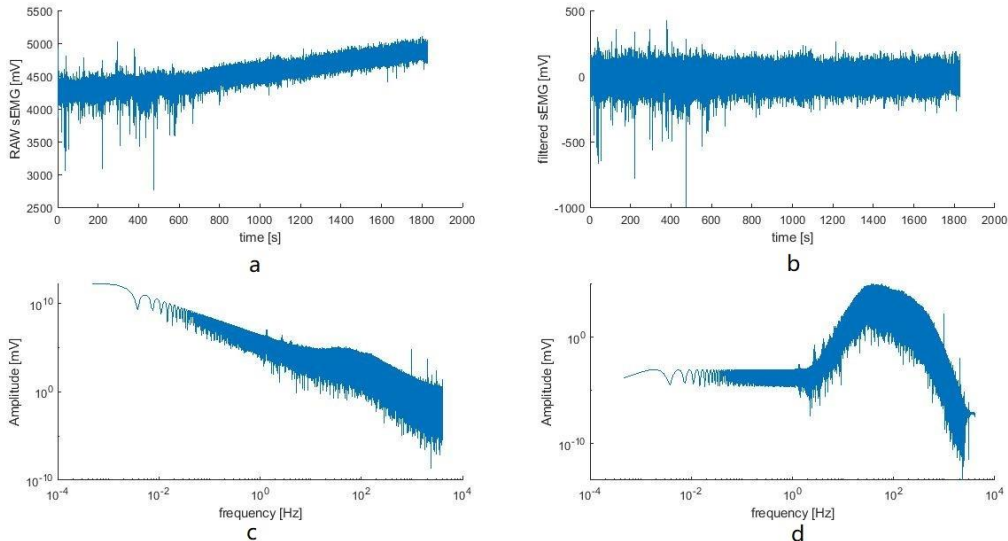


Figure 5.23 sEMG and power spectrum

In figure 5.24, the mean frequency and median frequency of the sEMG signal power spectrum are analyzed within 3 seconds, so there are $3 * 8k$ (samples per second) = 24 k data points. The analysis step is 1 second.

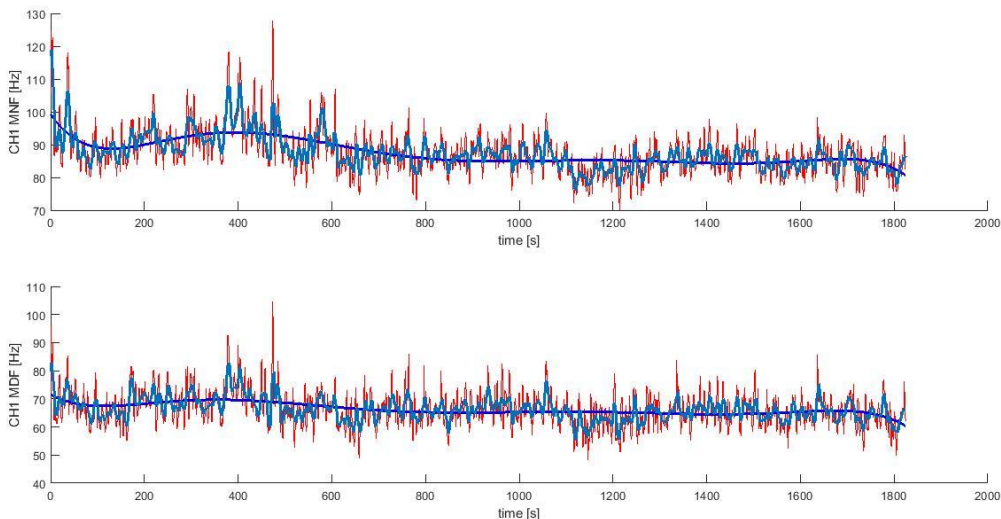


Figure 5.24 MNF and MDF, athlete 6

5.2.2.2. 25 min cycling (Athlete 7)

This athlete does physical exercise often, his rate of work is higher than athlete 6, and cycling time is shorter. The resistance level (18) and speed (80 RPM) are constant.

Figure 5.25 shows the raw sEMG and filtered sEMG signals during the experiment, the red line is the filtered sEMG signal.

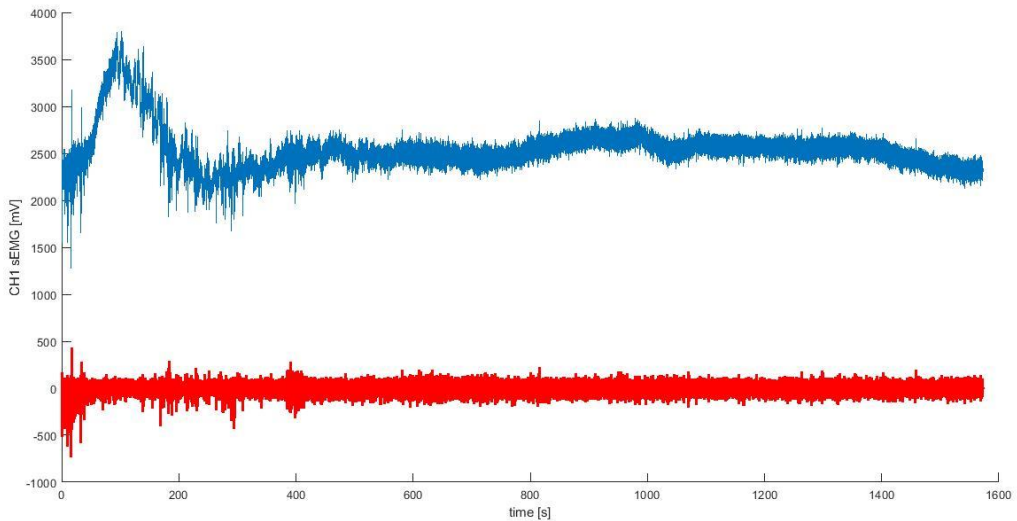


Figure 5.25 Raw sEMG and filtered sEMG

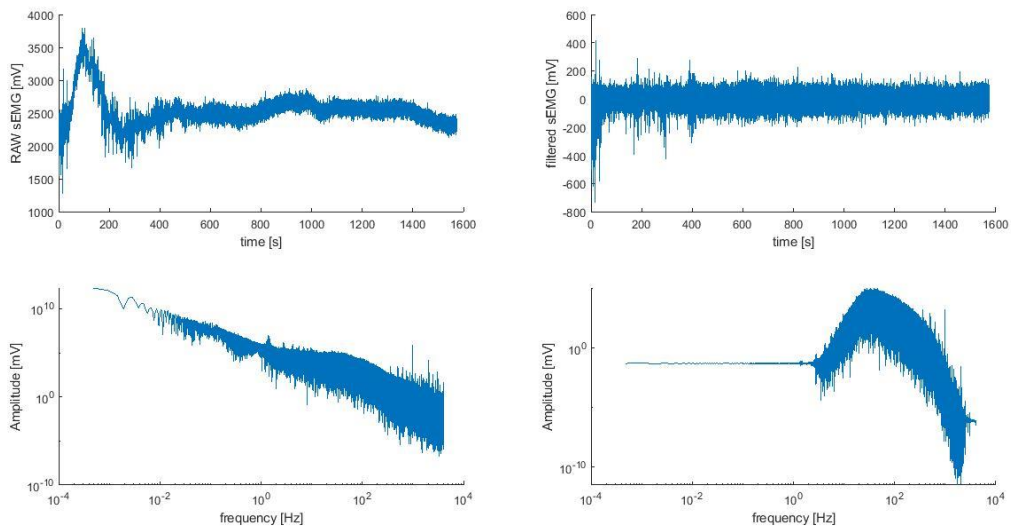


Figure 5.26 sEMG and power spectrum

In figure 5.27, the frequency analysis is performed on every 3 seconds of filtered sEMG data.

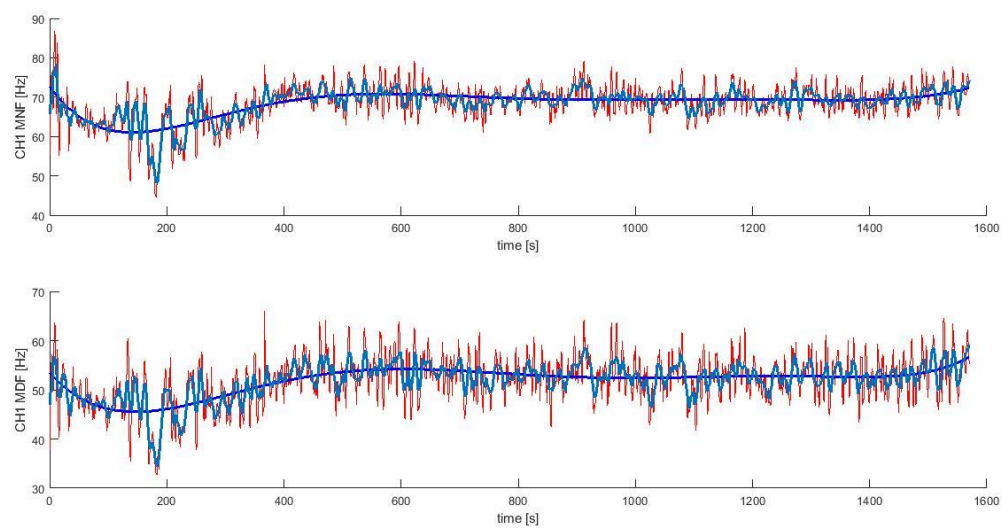


Figure 5.27 MNF and MDF, athlete 7

6. Discussions and Future Works

6.1. Discussions

In this thesis project, an sEMG detecting and recording system have been designed and built based on the related theories. The sEMG system fulfills the system requirements, it could be used to detect sEMG signals for analyzing local muscle fatigue, the indices of muscle fatigue are MNF/MDF, and MFPV decrease. The sampling rate is 8000 samples per second for 2 channels simultaneously, the ADC resolution is 24-bit, the noises could be reduced by the reference circuit and the digital filters. MNF/MDF analysis of isometric exercise shows a relation of the decrease in MNF/MDF and muscle fatigue.

There are some points for system improvement. First, the data rate could be improved. Second, the data transmission method could be wireless. Third, in the cycling exercise, the decrease in MNF and MDF are not clear to see when there is muscle fatigue. Fourth, the experiment preparation is very complicated and time-consuming, and the electrode-skin contact is not so good when the athlete sweats a lot. The details for improvement are in section 6.2.

6.2. Future works

6.2.1. Improvement of system performance

6.2.1.1. Sampling rate

The highest sampling rate of the ADS1299 chip could be 16000 SPS for 8 input channels simultaneously. If one channel records one muscle, sEMG signals from 8 muscles could be recorded and analyzed. This is useful for ergonomic studies. For example, when a football athlete kicks a ball, the thigh muscles, calf muscles, and waist muscles, etc. cooperate to complete this action. More input channels enable researchers to discover local muscle fatigue for more muscles, and the athlete could do targeted muscle training based on the analysis, in this way the sports injury could be reduced.

6.2.1.2. Data saving or transmission

If the data transmission speed is high enough, wireless data transmission or saving the data to an SD card should be possible. The microprocessor is integrated with Bluetooth and Wi-Fi. Wireless data transmission makes it possible for the researchers to see muscle performance without delay, so people could get warned when there is muscle fatigue, and the device could be made wearable.

6.2.2. Improvement of physiological experiment

6.2.2.1. Data collection

The collected data could be improved. Due to COVID-19, the gym was closed, and the experiment could not continue. 2 athletes participated in the cycling test, the decrease in MNF and MDF are not clear to see, and both athletes often do physical exercise. According to the results of the wall-sit experiment, the MNF and MDF decrease during isometric exercise is related to muscle condition, the decrease is more significant and happens earlier for the unfit athlete. So, if all the athletes did both isometric and isotonic exercise, the results (frequency shift) of both exercises from the same athlete could be compared, including the frequency maximum and minimum values, decreased percentage, experiment time. Then the researcher could get a clearer conclusion of the capability of using the sEMG system for muscle fatigue detection in dynamic exercise.

6.2.2.2. Experiment material

The electrodes that are used in the experiments are not very sticky, even with the elastic tapes applied on the electrodes, the connection is still not so good when the athlete sweats a lot. So, using more sticky wet electrodes may solve the connection problem. The electrode material should not lose their stickiness or react with sweat.

References

- [1] E. Verhagen, "The cost of sports injuries," *Journal of Science and Medicine in Sport*, vol. 13, pp. e40, 2010.
- [2] C. Thillou *et al.*, *Sensor-based mini-comedia*, 2014.
- [3] Merriam-Webster. "Electrogram," accessed 24-10-2019; <https://www.merriam-webster.com/dictionary/electrogram>.
- [4] LEXICO. "EKG," accessed 24-10-2019; <https://en.oxforddictionaries.com/definition/EKG>.
- [5] M. Bresadola, "Medicine and science in the life of Luigi Galvani (1737–1798)," *Brain Research Bulletin*, vol. 46, no. 5, pp. 367-380, 1998/07/15/, 1998.
- [6] B. C. i. C. E. Du Bois Reymond E (1849) Untersuchungen über thierische Elektikstät. Vol 2:425–30. (G Reimer, O'Malley CD. The human brain and spinal cord: a historical study, 2nd ed. San Francisco: Norman, 1996:192–203.
- [7] T. S. Physiologist. "Online Cardiology Resource," accessed 13-12-2019; <https://thephysiologist.org/study-materials/the-ecg-leads-polarity-and-einthovens-triangle/>.
- [8] WIKIPEDIA. "Einthoven's triangle," accessed 03-04-2019; https://en.wikipedia.org/wiki/Einthoven%27s_triangle.
- [9] J. Erlanger, and H. S. Gasser, *Electrical Signs of Nervous Activity*: University of Pennsylvania Press, 1937.
- [10] Britannica. "Muscle," accessed 10-12-2019; <https://www.britannica.com/science/muscle>.
- [11] D. A. Winter, *Biomechanics and Motor Control of Human Movement*, Fourth Edition ed., University of Waterloo, Waterloo, Ontario, Canada: John Wiley & Sons, Inc., 2009.
- [12] Britannica. "Sarcomere," accessed 06-12-2019; <https://www.britannica.com/science/sarcomere>.
- [13] E. R. D. Gordon, Graham E. Caldwell, Joseph Hamill, Gary Kamen, Saunders N. Whittlesey, "Research Methods in Biomechanics," *Journal of Sports Science & Medicine*, vol. 13, no. 1, pp. i-i, 2014.
- [14] S. Ward. "THE HUMAN CELL ATLAS: AN INTERNATIONAL EFFORT," accessed 10-10-2019; <http://altox.org/the-human-cell-atlas-an-international-effort/>.
- [15] G. R. (n.d.). "Human Physiology-Neurons & the Nervous System," accessed 12-02-2019; <http://people.eku.edu/ritchisong/301notes2.htm>.
- [16] R. M. (n.d.). "Muscles," accessed 15-02-2019; <https://www.slideserve.com/raoul/muscles>.
- [17] WIKIPEDIA. "Skeletal muscle," accessed 11-02-2019; https://en.wikipedia.org/wiki/Skeletal_muscle#/media/File:Blausen_0801_SkeletalMuscle.png.
- [18] L. M. Mendell, "The size principle: a rule describing the recruitment of motoneurons," *Journal of Neurophysiology*, vol. 93, no. 6, pp. 3024-3026, 2005.
- [19] S. (n.d.). "Neuronal Physiology," accessed 19-02-2019; <https://www.studyblue.com/notes/note/n/chapter-4-neuronal-physiology/deck/722174>.
- [20] A. B. M. H. (n.d.). "Cell Membrane," accessed 18-02-2018; <https://socratic.org/questions/what-are-the-main-functions-of-the-cell-membrane>.
- [21] P. (n.d.). "Formation Of An Action Potential - Action Potential Steps," accessed 09-12-2019; https://www.pngkey.com/detail/u2w7e6r5u2a9i1r5_formation-of-an-action-potential-action-potential-steps/.

- [22] P. V. Komi, and E. R. Buskirk, "Reproducibility of electromyographic measurements with inserted wire electrodes and surface electrodes," *Electromyography*, vol. 10, no. 4, pp. 357-67, Nov-Dec, 1970.
- [23] "Biopotentials 2019," accessed 16-03-2019; <https://www.ele.uri.edu/courses/bme362/handouts/Biopotentials.pdf>.
- [24] S. C. P. R. Wotiz (PhD '06), B. Cole (PhD '12), B. Toba (MS '07), J. Lin (MS '08), and P. C. D. L. B. n. d. Prof. S. Hamid Nawab. "Muscles Alive," accessed 08-10-2018; www.bu.edu/ids/research-projects/muscles-alive/.
- [25] N. A. Dimitrova, and G. V. Dimitrov, "Interpretation of EMG changes with fatigue: facts, pitfalls, and fallacies," *J Electromyogr Kinesiol*, vol. 13, no. 1, pp. 13-36, Feb, 2003.
- [26] D. Somerset. "Neural Tuning for Improving Strength: Pre/Post Activation Sequencing," accessed 19-11-2018; <https://deansomerset.com/neural-tuning-improving-strength-prepost-activation-sequencing/>.
- [27] M. Cifrek *et al.*, "Surface EMG based muscle fatigue evaluation in biomechanics," *Clinical Biomechanics*, vol. 24, no. 4, pp. 327-340, 2009/05/01/, 2009.
- [28] C. J. Rebouche, and A. G. Engel, "Carnitine metabolism and deficiency syndromes," *Mayo Clinic proceedings*, vol. 58, no. 8, pp. 533-540, 1983/08//, 1983.
- [29] J. P. Braakhekke, D. F. Stegeman, and E. M. G. Joosten, "Increase in median power frequency of the myoelectric signal in pathological fatigue," *Electroencephalography and Clinical Neurophysiology*, vol. 73, no. 2, pp. 151-156, 1989/08/01/, 1989.
- [30] S. Thongpanja *et al.*, "Mean and Median Frequency of EMG Signal to Determine Muscle Force Based on Time-Dependent Power Spectrum," *Elektronika ir Elektrotehnika*, vol. 19, pp. 51-56, 03/01, 2013.
- [31] A. Searle, and L. Kirkup, "A direct comparison of wet, dry and insulating bioelectric recording electrodes," *Physiological Measurement*, vol. 21, no. 2, pp. 271-283, 2000/05/01, 2000.
- [32] J. G. e. Webster, *Medical instrumentation: application and design*, 4th ed., Hoboken, NJ: John Wiley & Sons, 2010.
- [33] PLUX. "Biosignalsplux wearable body sensing platform," accessed 20-10-2019; <https://www.biosignalsplux.com/index.php>.
- [34] PLUX. "Biosignalsplux wearable body sensing platform," accessed 18-11-2019; <https://www.biosignalsplux.com/index.php/biofeedback-rehabilitation>.
- [35] Ceracarta. "Electrode," accessed 27-01-2020, ; <http://www.ceracarta.it/elettrodi/#ecg>.
- [36] J. W. R Porter, "Human muscle fatigue: physiological mechanisms," *Ciba Found Symp*, vol. 82, pp. 1-314, 1981.
- [37] P. J. A. p. i. t. k. e. Konrad, "The abc of emg," vol. 1, no. 2005, pp. 30-5, 2005.
- [38] A. M. (n.d.). "The Benefits of the Wall Sit: Under Estimated Lower Body Exercise," accessed 03-01-2010; <https://athleticmuscle.net/wall-sit/>.
- [39] G. J. B. M. Eric H. Awtry MD. "Exercise and the Heart," accessed 01-02-2020; <https://www.sciencedirect.com/topics/medicine-and-dentistry/isotonic-exercise>.
- [40] T. INSTRUMENTS. "ADS1299-x Low-Noise, 4-, 6-, 8-Channel, 24-Bit, Analog-to-Digital Converter for EEG and Biopotential Measurements," <http://www.ti.com/lit/ds/sbas499c/sbas499c.pdf?&ts=1590120282944>.

APPENDIX-A

Circuit diagrams

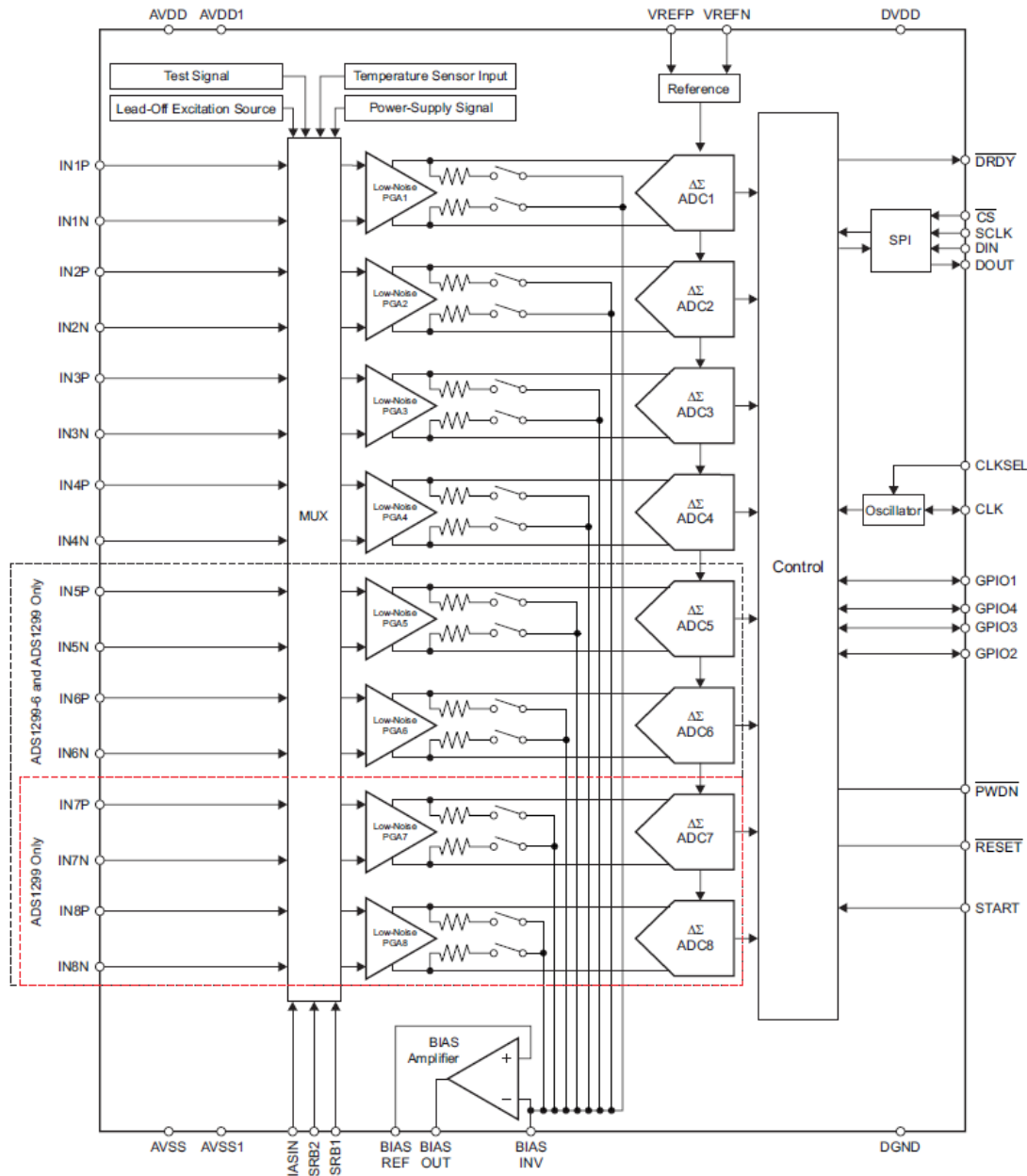


Figure 1 Circuit diagram of chip ADS1299[1]

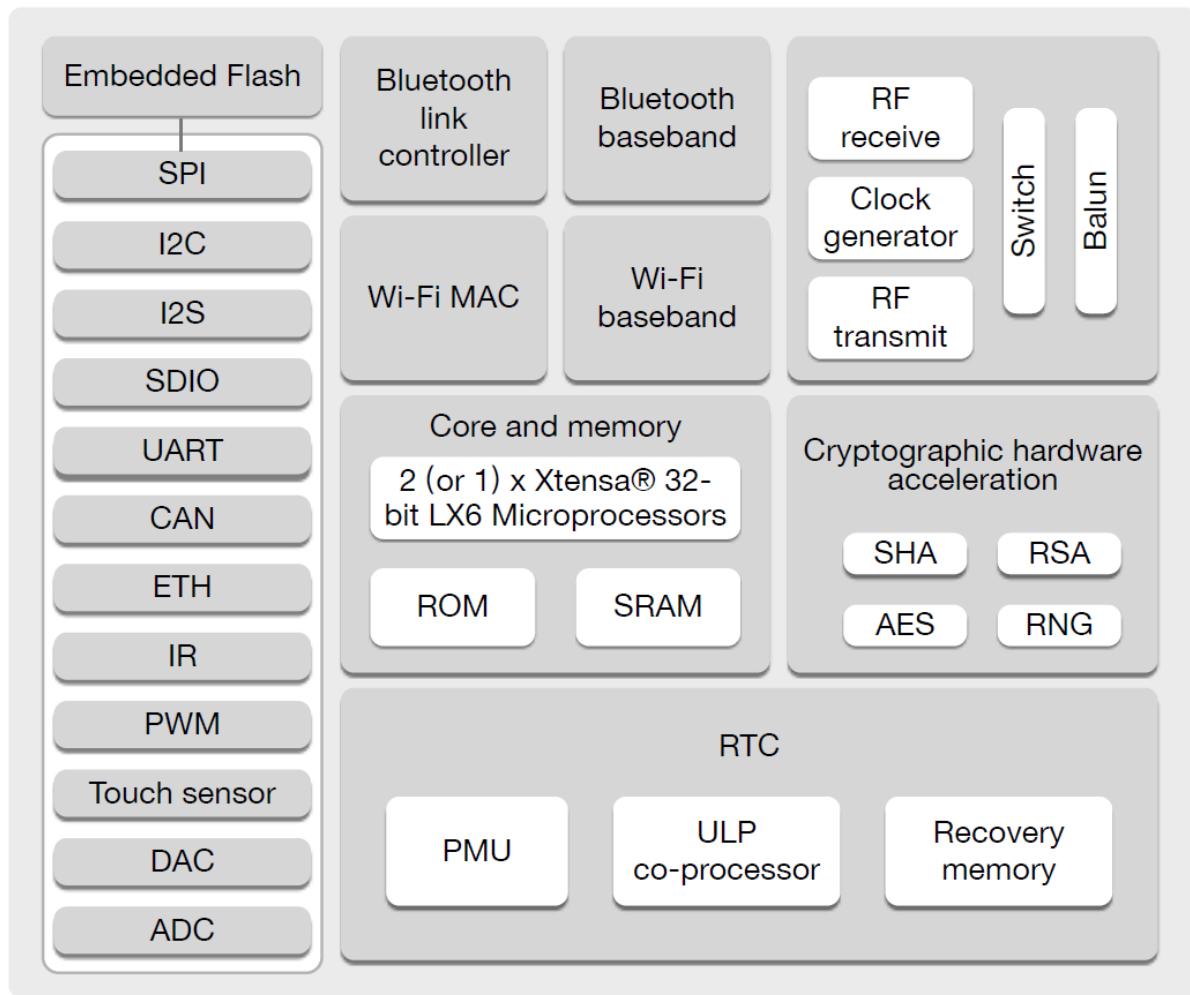


Figure 1 Block diagram of the ADS1299 evaluation board[2]

References:

- [1] TEXAS INSTRUMENTS, 2017, ADS1299-x Low-Noise, 4-, 6-, 8-Channel, 24-Bit, Analog-to-Digital Converter for EEG and Biopotential Measurements, <http://www.ti.com/lit/ds/sbas499c/sbas499c.pdf?&ts=1590120282944>.
- [2] TEXAS INSTRUMENTS, 2016, EEG Front-End Performance Demonstration Kit, <http://www.ti.com/lit/ug/slau443b/slau443b.pdf?&ts=1590123099168>.

APPENDIX-B

Protocol for the physiological experiment

1. Introduction and objectives

The aim of this experiment is to find out if the EMG system that I built can detect muscle fatigue by measuring a decrease in MPF and MFPV.

1. If the mean power spectrum frequency (MPF) shifts towards lower value, it can be concluded that there is muscle fatigue.
2. If muscle fiber propagation velocity (MFPV) decreases, it can be concluded that there is muscle fatigue.

2. Research questions

1. How good is the quality of the signal?
 - a. What is the frequency range of the signal?
2. Will the decreases in these two variables measurable? Do we see the shift?
 - a) How many shocks influence performance?
 - b) How does MPF or MFPV change in exercise?
3. Identify other disturbance factors.

3. Materials:

- sEMG measuring box

In the box there are ADS1299, ESP32 evaluation boards, and Micro SD card with shield, however, the SD card is not used in this experiment. ADS1299 does the analog-to-digital conversion to the sensed sEMG signals, ESP32 process, and transmit the digital signals.

- Wet electrodes
- Input cables
- USB cable
- Heart rate monitor —Polar Beat
- Tapes or elastic band for fixing the electrodes
- Scissors for cutting tapes
- Vaseline
- Smartphone with Polar Beat APP installed
- Battery-powered laptop with all the software installed

4. Methods

1. Fill in the survey with the athletes

Table 1. Questionnaire

Name or Number:			
gender		How often do you exercise?	
age		How long do you exercise each time?	
BMI		Which exercise do you usually do?	
Normal heart rate		High heart rate in exercise	

2. Keep the cycling speed constant during the experiment.

By doing this, the influence of changing muscle performance can be reduced. Since the cycling speed is controlled, the period of muscle contraction is controlled.

3. The data will be recorded during the experiment.

- a) sEMG signals are recorded in a file saved on the laptop through a serial port, the start time of recording will be recorded as well.
- b) The heart rate is recorded by the heart rate monitor – Polar Beat, the data could be downloaded later from a website.
- c) The position of electrodes is recorded by a smartphone camera.

4. The data will be read out in MATLAB after the experiment.

The recorded sEMG data are in text file format, which can be easily read out and processed by MATLAB.

5. Uncertainties

1. Wet electrodes become not adhesive during exercises because of sweat.

Use tapes to adjust electrodes when necessary

2. Applying tape or elastic bands on the electrodes causes signal changes.

Compare the results, find possible influences.

3. Noises like 1/f noise, power line noise, and the cable motion artifact, movement artifact, baseline noise.

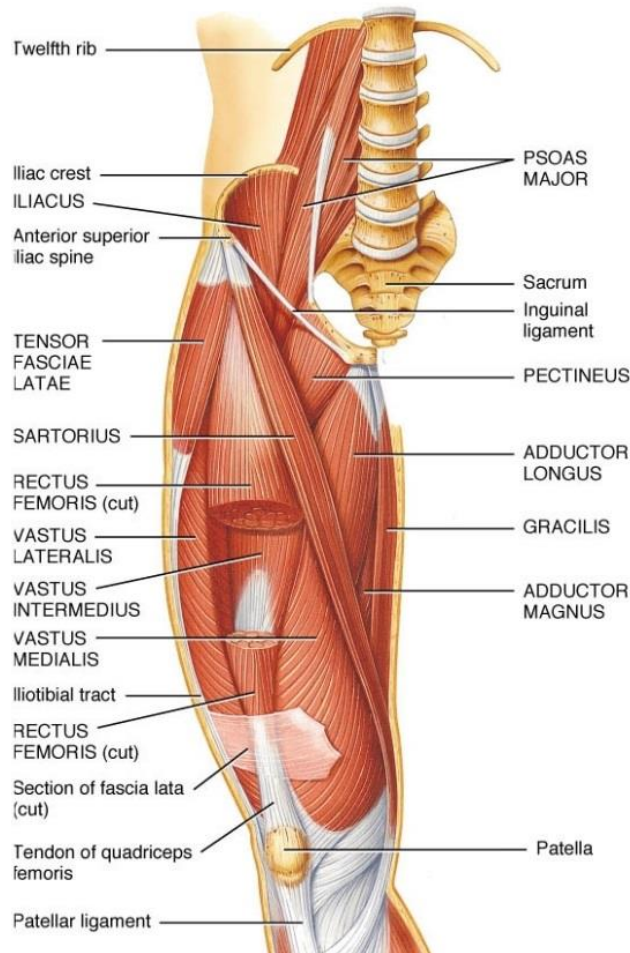
- a) Do digital filtering to the raw sEMG signal to eliminate 1/f noise.
- b) The power line noise, 50Hz AC main noise is reduced by a reference electrode in the sEMG system, and the system is powered by battery only. The cable motion artifact can be reduced by proper circuit design.
- c) Muscle moves relative to the skin during exercises cause the movement artifact noise. The muscle fiber propagation velocity analysis is affected because the signals

are sensed on the skin rather than in the muscle. Do stationary exercise could reduce the influence of this movement.

- d) Baseline noise

6. Procedure

1. Ask the participants to do skin preparation and fill out the form beforehand, get all the materials ready.
2. Do stationary exercise.
 - a) Check skin preparation and required materials.
 - b) Let participants find positions for electrodes. The electrodes should measure sEMG signals from Vastus Medialis. Refer to figures 1-3 to find the positions.



(a) Anterior superficial view

Figure 1. Anterior superficial view of Quadriceps Femoris [1]

Recommendations for sensor locations in hip or upper leg muscles

Muscle	
Name	Quadriceps Femoris
Subdivision	vastus medialis
Muscle Anatomy	
Origin	Distal half of the intertrochanteric line, medial lip of line aspera, proximal part of medial supracondylar line, tendons of adductor longus and adductor magnus and medial intermuscular septum.
Insertion	Proximal border of the patella and through patellar ligament.
Function	Extension of the knee joint.
Recommended sensor placement procedure	
Starting posture	Sitting on a table with the knees in slight flexion and the upper body slightly bend backward.
Electrode size	Maximum size in the direction of the muscle fibres: 10 mm.
Electrode distance	20 mm.
Electrode placement	
- location	Electrodes need to be placed at 80% on the line between the anterior spina iliaca superior and the joint space in front of the anterior border of the medial ligament.
- orientation	Almost perpendicular to the line between the anterior spina iliaca superior and the joint space in front of the anterior border of the medial ligament.
- fixation on the skin	(Double sided) tape / rings or elastic band.
- reference electrode	On / around the ankle or the proc. spin. of C7.
Clinical test	Extend the knee without rotating the thigh while applying pressure against the leg above the ankle in the direction of flexion.
Remarks	The SENIAM guidelines include a separate sensor placement procedure for the vastus lateralis and the rectus femoris muscle.

Figure 2. Recommendations for sensor locations

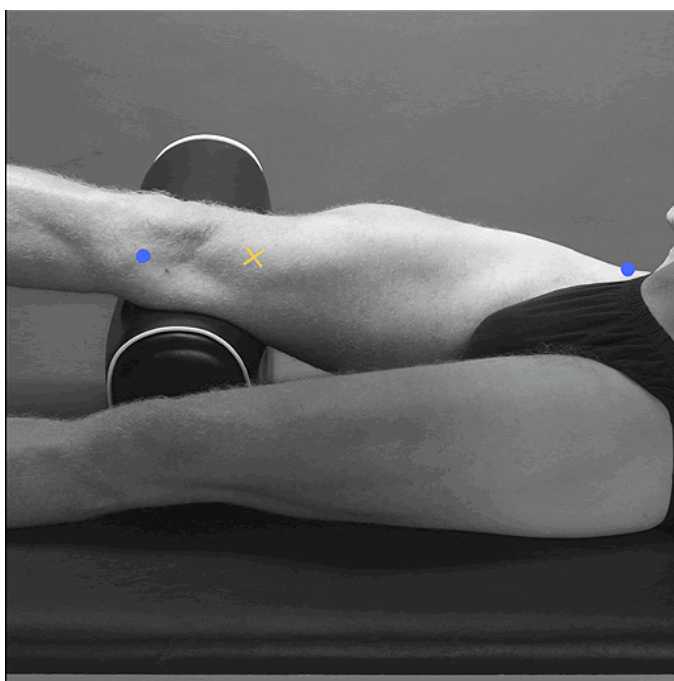


Figure3. Start position for Quadriceps Femoris electrodes placement

As shown in figure 3, at the cross sign put the two input electrodes in the direction along with the muscle, at either blue point put the reference electrode.

c) Test connection

Ask the participant to do a contraction and see sEMG signal waveform on the laptop

d) Find appropriate foot position for wall-sit



Figure 4. Wall-sit

The participant should not move during the test, the angle of Thighs and calves should be 90 degrees.

- e) Start recording sEMG, heart rate, time
 - f) Ensure connection during tests. The test should be 100s or longer.
Tapes are not necessary because of the short period. There is not much sweat.
 - g) Complete the test, remove the electrodes, let the athletes relax for 30 min.
3. The dynamic exercise 1, Leg press
The leg press can be used to develop the quadriceps and hamstrings of the thigh. The advantage of doing this exercise in the experiment is that fewer muscles are enrolling in leg press compared with cycling, however, the speed of doing leg press cannot be controlled, therefore the power cannot be controlled, additionally, it is difficult for beginners to use the leg press machine correctly.
4. The dynamic exercise 2, cycling
Compared to running, cycling is easier for the researcher to check the connection, and electrodes are less likely to fall off because of gravity and sweat.
- a) Perform an estimation for each athlete.
 - a. 5 minutes warming up.
 - b. Perform estimation for 5 min. Set the resistance level to 10-13, this is determined by the athlete, and let the athlete keep cycling at 80 RPM. The resistance level is increased every 30 seconds until the athlete could not cycle at 80 RPM for 30 seconds.
 - b) Do preparation as 2.a b c d, ensure that the participants are in good muscle condition. In the meantime, the athlete rest for over 15 minutes.

Use tapes in advance to prevent electrodes from falling off. Apply a small amount of Vaseline between the electrodes to prevent input short. Too much Vaseline could cause viscosity to reduce of the electrodes.

- c) 2 minutes warming up
 - d) Let athletes cycle on cycling machines and start recording data
 - e) Set speed as 80 rpm, the target time is 30 minutes, set resistance level as 2 levels lower than the maximum estimation level.
Keep cycling until the cadence drops to lower than $(1-10\%)*80 \text{ RPM} = 72 \text{ RPM..}$
 - f) Complete the test, remove the electrodes.
5. Thank the participants
 6. Data analysis

Raw data is processed with MATLAB

References:

- [1]. Bone and Spine. n.d. Muscles of hip, accessed 02-04-2020,
<https://boneandspine.com/muscles-of-hip/>

APPENDIX-C

Arduino-ESP32 source code

(Arduino 1.8.9)

1. Pin connection

```
/* connect the ESP32-DevKitC and ADS1299EEG FE printed circuit board (PCB), Rev A  
modules
```

```
ADS1299EEG FE | ESP32-DevKitC  
JP24 bottom 3.3V 11  
JP4 right 5V 119  
J3 4 GND GND r1  
J3 11 DIN IO23 MOSI r2  
J3 3 CLK IO18 SCK r9  
J3 7 CS IO5(17) SS r10  
J3 13 DOUT IO19 MISO r8  
J3 DRDY IO14  
J3 START IO13
```

```
/*
```

Connect the SD card to the following pins:

```
SD Card | ESP32
```

```
D2 -  
D3 SS  
CMD MOSI  
VSS GND  
VDD 3.3V  
CLK SCK  
VSS GND  
D0 MISO  
D1 -
```

```
*/
```

2. Read and write register functions

```
//write one register at one time  
void ads_wreg(char _address, char _value) {  
    char opcode1 = _WREG + _address;          //010r rrrr; _WREG 010r rrrr (4xh) & 000n nnnn  
    digitalWrite(CS, LOW);                  //Low to communicated  
    hspi->beginTransaction(SPISettings(spiClk, MSBFIRST, SPI_MODE1));  
  
    hspi->transfer(_SDATAC);           //SDATAC
```

```

hspi->transfer(opcode1);           //WREG address
hspi->transfer(0x00);             //number of register = 1, n nnnn=1-1=0
hspi->transfer(_value);
hspi->transfer(_RDATAC);          //turn read data continuous back on
hspi->endTransaction();

digitalWrite(CS , HIGH);           //High to end communication
delay(0.001);                     // WAIT 2*TCLK'S = 888ns = 1us
}

//hspi command _RREW.... no delay
void ads_command(char _cmd) {
    hspi->beginTransaction(SPISettings(spiClk, MSBFIRST, SPI_MODE1));
    digitalWrite(CS , LOW);           //Low to communicated
    hspi->transfer(_cmd);
    digitalWrite(CS , HIGH);          //High to end communication
    hspi->endTransaction();
}

//read one register at one time
void ads_rreg(char _address) {
    hspi->beginTransaction(SPISettings(spiClk, MSBFIRST, SPI_MODE1));
    char opcode1 = _RREG + _address;   //001r rrrr; _RREG 001r rrrr (2xh) & 000n nnnn
    digitalWrite(CS , LOW);           //Low to communicated
    hspi->transfer(_SDATAC);         //SDATAC
    hspi->transfer(opcode1);         //RREG address
    hspi->transfer(0x00);            //number of register = 1, n nnnn=1-1=0
    byte temp = hspi->transfer(0x00);
    digitalWrite(CS , HIGH);          //High to end communication
    hspi->endTransaction();
    Serial.println(temp, HEX);
    delay(0.001);
}

//pull reset pin low for 2us or use RESET cmd
void ads_pwr_up_seq()
{
    delay(40);          // WAIT 40ms
    ads_command(_RESET);
    delay(0.0012);      // WAIT 12us
}

```

3. Serial Read 1-channel output data from ADS1299

```
#include <SPI.h>
#include "ads1299.h"
```

```

const int DRDY = 17; //data ready pin
//const int START = 13; //data ready pin
const int CS = 15;

const float tCLK = 0.000666;
static const int spiClk = 9000000; // 9 MHz

// uninitialized pointers to SPI objects
SPIClass * hspi = NULL;

void setup() {
    //initialise two instances of the SPIClass attached to VSPI and HSPI respectively

    Serial.begin(2000000);

    Serial.println("ADS1299-bridge has started!");

    pinMode(CS, OUTPUT); //HSPI SS

    // initailize the data ready and chip select pins:
    pinMode(DRDY, INPUT);
    // pinMode(START, OUTPUT);
    // digitalWrite(START , LOW);
    hspi = new SPIClass(HSPI);
    hspi->begin();
    ads_pwr_up_seq();
    ads_wreg(CONFIG1, 0x90);      //CONFIG1 96h Default 250sps, 91h 8 kSPS
    ads_wreg(CONFIG2, 0xD0);      //CONFIG2 C0h Deafault,10 normal input,D0 test signal
generated internally
    ads_wreg(CONFIG3, 0xEE);      //CONFIG3 E0h for internal reference
    ads_wreg(LOFF, 0x02);
    ads_wreg(CH1SET,   ADS1299_PGA_GAIN01 | ADS1299_INPUT_NORMAL | ADS1299_INPUT_PWR_UP);
    ads_wreg(CH2SET,   ADS1299_PGA_GAIN01 | ADS1299_INPUT_SUPPLY | ADS1299_INPUT_PWR_DOWN);
    ads_wreg(CH3SET,   ADS1299_PGA_GAIN01 | ADS1299_INPUT_SUPPLY | ADS1299_INPUT_PWR_DOWN);
    ads_wreg(CH4SET,   ADS1299_PGA_GAIN01 | ADS1299_INPUT_SUPPLY | ADS1299_INPUT_PWR_DOWN);
    ads_wreg(CH5SET,   ADS1299_PGA_GAIN01 | ADS1299_INPUT_SUPPLY | ADS1299_INPUT_PWR_DOWN);
    ads_wreg(CH6SET,   ADS1299_PGA_GAIN01 | ADS1299_INPUT_SUPPLY | ADS1299_INPUT_PWR_DOWN);
    ads_wreg(CH7SET,   ADS1299_PGA_GAIN01 | ADS1299_INPUT_SUPPLY | ADS1299_INPUT_PWR_DOWN);
    ads_wreg(CH8SET,   ADS1299_PGA_GAIN01 | ADS1299_INPUT_SUPPLY | ADS1299_INPUT_PWR_DOWN);

```

```

// digitalWrite(START , LOW);      //Activate Conversion.After This Point DRDY Toggles
at
// fCLK / 8192

Serial.println("SPI configured \n");

delay(10); //delay to ensure connection

}

void loop() {
    long ch1;

//START conversion
digitalWrite(CS , LOW);
hspi->transfer(_START);
digitalWrite(CS , HIGH);

while (1) {
    while (digitalRead(DRDY) == HIGH) {

    }

if (digitalRead(DRDY) == LOW) {
    digitalWrite(CS , LOW);
    hspi->transfer(_RDATAAC);
    long dataPacket;
    for (int i = 0; i < 2; i++) {
        for (int j = 0; j < 3; j++) {
            byte dataByte = hspi->transfer(0x00);
            dataPacket = (dataPacket << 8) | dataByte;
        }
        if (i == 1) {
            ch1 = dataPacket;
        }
        dataPacket = 0;
    }

    digitalWrite(CS , HIGH);
    Serial.println(ch1);
    hspi->endTransaction();
}

}

}

```

4. Serial Read 2-channel output data from ADS1299

```
#include <SPI.h>
#include "ads1299.h"

const int DRDY = 17; //data ready pin
//const int START = 13; //data ready pin
const int CS = 15;

const float tCLK = 0.000666;
static const int spiClk = 9000000; // 9 MHz

//uninitialized pointers to SPI objects
SPIClass * hspi = NULL;

void setup() {
    //initialise two instances of the SPIClass attached to VSPI and HSPI respectively
    Serial.begin(2000000);

    Serial.println("ADS1299-bridge has started!");

    pinMode(CS, OUTPUT); //HSPI SS

    // initialize the data ready and chip select pins:
    pinMode(DRDY, INPUT);
    // pinMode(START, OUTPUT);
    // digitalWrite(START, LOW);
    hspi = new SPIClass(HSPI);
    hspi->begin();
    ads_pwr_up_seq();
    ads_wreg(CONFIG1, 0x91);      //CONFIG1 96h Default 250sps, 91h 8 kSPS
    ads_wreg(CONFIG2, 0xD0);      //CONFIG2 C0h Deafault, D0 test signal generated
internally
    ads_wreg(CONFIG3, 0xEE);      //CONFIG3 E0h for internal reference
    ads_wreg(LOFF, 0x02);
    ads_wreg(CH1SET,   ADS1299_PGA_GAIN01 | ADS1299_INPUT_NORMAL | ADS1299_INPUT_PWR_UP);
    ads_wreg(CH2SET,   ADS1299_PGA_GAIN01 | ADS1299_INPUT_NORMAL | ADS1299_INPUT_PWR_UP);
    ads_wreg(CH3SET,   ADS1299_PGA_GAIN01 | ADS1299_INPUT_SUPPLY | ADS1299_INPUT_PWR_DOWN);
    ads_wreg(CH4SET,   ADS1299_PGA_GAIN01 | ADS1299_INPUT_SUPPLY | ADS1299_INPUT_PWR_DOWN);
```

```

ads_wreg(CH5SET,    ADS1299_PGA_GAIN01 | ADS1299_INPUT_SUPPLY | 
ADS1299_INPUT_PWR_DOWN);
ads_wreg(CH6SET,    ADS1299_PGA_GAIN01 | ADS1299_INPUT_SUPPLY | 
ADS1299_INPUT_PWR_DOWN);
ads_wreg(CH7SET,    ADS1299_PGA_GAIN01 | ADS1299_INPUT_SUPPLY | 
ADS1299_INPUT_PWR_DOWN);
ads_wreg(CH8SET,    ADS1299_PGA_GAIN01 | ADS1299_INPUT_SUPPLY | 
ADS1299_INPUT_PWR_DOWN);

// digitalWrite(START , LOW);      //Activate Conversion.After This Point DRDY Toggles
at
// fCLK / 8192

Serial.println("SPI configured \n");

delay(10); //delay to ensure connection

}

void loop() {
    long ch1;
    long ch2;
//START conversion
digitalWrite(CS , LOW);
hspi->transfer(_START);
digitalWrite(CS , HIGH);

while (1) {
    while (digitalRead(DRDY) == HIGH) {

    }

if (digitalRead(DRDY) == LOW) {
    digitalWrite(CS , LOW);
    hspi->transfer(_RDATAc);
    long dataPacket;
    for (int i = 0; i < 3; i++) {
        for (int j = 0; j < 3; j++) {
            byte dataByte = hspi->transfer(0x00);
            dataPacket = (dataPacket << 8) | dataByte;
        }
        if (i == 1) {
            ch1 = dataPacket;
        }
        else if (i == 2) {
            ch2 = dataPacket;
        }
        dataPacket = 0;
    }
}
}

```

```

digitalWrite(CS , HIGH);
Serial.printf("%d,%d\n", ch1, ch2);
hspi->endTransaction();
}

}

```

5. Read data to SD card

```

#include <SPI.h>
#include "ads1299.h"
#include "SDcmd.h"
#include <stdlib.h>
#include <stdio.h>
#include <string.h>

const int DRDY = 17; //data ready pin
//const int START = 13; //data ready pin
const int CS = 15;

const float tCLK = 0.000666;
static const int spiClk = 9000000; // 10 MHz

//uninitialised pointers to SPI objects
SPIClass * hspi = NULL;
SPIClass * vspi = NULL;

void setup() {
  //initialise two instances of the SPIClass attached to VSPI and HSPI respectively

  Serial.begin(2000000);

  if (!SD.begin()) {
    Serial.println("Card Mount Failed");
    return;
  }
  createDir(SD, "/ads1299");
  writeFile(SD, "/ads1299/signal.txt", "sEMG\n");

  Serial.println("ADS1299-bridge has started!");

  pinMode(CS, OUTPUT); //HSPI SS

  // initialize the data ready and chip select pins:

```

```

pinMode(DRDY, INPUT);
// pinMode(START, OUTPUT);
// digitalWrite(START , LOW);
hspi = new SPIClass(HSPI);
hspi->begin();
ads_pwr_up_seq();
ads_wreg(CONFIG1, 0x91);      //CONFIG1 96h Default 250sps, 91h 8 kSPS
ads_wreg(CONFIG2, 0xD0);      //CONFIG2 C0h Deafault, D0 test signal generated
internally
ads_wreg(CONFIG3, 0xCE);      //CONFIG3 E0h for internal reference
ads_wreg(LOFF, 0x02);
ads_wreg(CH1SET,   ADS1299_PGA_GAIN01 | ADS1299_INPUT_TESTSIGNAL | 
ADS1299_INPUT_PWR_UP);
ads_wreg(CH2SET,   ADS1299_PGA_GAIN01 | ADS1299_INPUT_TESTSIGNAL | 
ADS1299_INPUT_PWR_UP);
ads_wreg(CH3SET,   ADS1299_PGA_GAIN01 | ADS1299_INPUT_TESTSIGNAL | 
ADS1299_INPUT_PWR_UP);
ads_wreg(CH4SET,   ADS1299_PGA_GAIN01 | ADS1299_INPUT_SUPPLY | 
ADS1299_INPUT_PWR_DOWN);
ads_wreg(CH5SET,   ADS1299_PGA_GAIN01 | ADS1299_INPUT_SUPPLY | 
ADS1299_INPUT_PWR_DOWN);
ads_wreg(CH6SET,   ADS1299_PGA_GAIN01 | ADS1299_INPUT_SUPPLY | 
ADS1299_INPUT_PWR_DOWN);
ads_wreg(CH7SET,   ADS1299_PGA_GAIN01 | ADS1299_INPUT_SUPPLY | 
ADS1299_INPUT_PWR_DOWN);
ads_wreg(CH8SET,   ADS1299_PGA_GAIN01 | ADS1299_INPUT_SUPPLY | 
ADS1299_INPUT_PWR_DOWN);

// digitalWrite(START , LOW);      //Activate Conversion.After This Point DRDY Toggles
at
// fCLK / 8192

Serial.println("SPI configured \n");

delay(10); //delay to ensure connection

}

void loop() {

//START conversion
digitalWrite(CS , LOW);
hspi->transfer(_START);
digitalWrite(CS , HIGH);

while (1) {
    while (digitalRead(DRDY) == HIGH) {

}

```

```

if (digitalRead(DRDY) == LOW) {
    digitalWrite(CS , LOW);
    hspi->transfer(_RDATA_C);

    for (int i = 0; i < 4; i++) {
        for (int j = 0; j < 3; j++) {
            char dataByte = hspi->transfer(0x00);
            Serial.write(dataByte);
        }
        //      if (i == 0) {
        //          Serial.write(",");
        //      }
        //      else if (i == 1) {
        //          Serial.write(",");
        //      }
        //      else if (i == 2) {
        //          Serial.write(",");
        //      }
        //      else if (i == 3) {
        if (i == 3) {
            Serial.write("\r");
            Serial.write("\n");
        }
        else {
            Serial.write(",");
        }
    }

    digitalWrite(CS , HIGH);
    hspi->endTransaction();
}

}

```

APPENDIX-D

Serial monitor

(Processing 3.3.7)

```
import processing.serial.*;  
  
Serial myPort; // Create object from Serial class  
PrintWriter myFile;  
  
void setup()  
{  
    printArray(Serial.list());  
    // Open the port you are using at the rate you want:  
    myFile = createWriter("filename.csv"); //Please change filename before running this program,  
    otherwise the existing file will be covered. File format could be txt, dat, csv...  
    size(200, 200);  
    // COM4 connected to ESP32, the 3rd serial port  
    String portName = Serial.list()[2]; //the 3rd serial port of this computer is occupied by the  
    device  
    myPort = new Serial(this, portName, 2000000);  
  
}  
  
void draw()  
{  
    if (myPort.available() > 0) {  
        String inBuffer = myPort.readString();  
        if (inBuffer != null) {  
            myFile.print(inBuffer);  
        }  
    }  
}  
  
void keyPressed() { //  
    myFile.flush(); // Writes the remaining data to the file  
    myFile.close(); // Finishes the file  
    println("Saving into \"myFile\" has been DONE!");  
    println();  
    exit(); // Stops the program  
}
```

APPENDIX-E

Data processing

(MATLAB R2018b)

1. Import data

```
%%import data
%02-12-2019
%\...\ codes\serial_read\filename.csv

clear
close all
clc

filename = '\...\ codes\serial_read\filename.csv';

RAW = csvread(filename,50,0);

RAW1 = RAW(:,1);

n = length (RAW1);
for i = 1 : n

    if RAW1(i)>= 16777218           %detect wrong data and plot
        i, RAW1(i)
    end

end
for i = 1 : n-1
    if RAW1(i+1)-RAW1(i)>= 8388608      %detect and repair ADC overflow
        RAW1(i+1) = RAW1(i+1)-16777216;
        i = i - 1;
    end
    if RAW1(i+1)-RAW1(i)<= -8388608
        RAW1(i+1) = RAW1(i+1)+16777216;
        i = i - 1;
    end
end

RAW2 = RAW(:,2);
n = length (RAW2);
for i = 1 : n
    if RAW2(i)>= 16777218
        i, RAW2(i)
    end
end
for i = 1 : n-1
    if RAW2(i+1)-RAW2(i)>= 8388608
```

```

        RAW2(i+1) = RAW2(i+1)-16777216;
        i = i - 1;
    end
    if RAW2(i+1)-RAW2(i)<= -8388608
        RAW2(i+1) = RAW2(i+1)+16777216;
        i = i - 1;
    end
end

```

2. Plot samples and filtered samples

```

%% plot CH1
Fs=8000;

RAW1 = RAW1 .* 9000/(2^24)/24;      %convert ADC output values to voltage
RAW2 = RAW2 .* 9000/(2^24)/24;

N1=length(RAW1);                  %number of RAW sEMG data point
n=0:N1-1;
t=n/Fs;
% RAW = abs (RAW);
figure
plot (t,RAW1), box off, hold on, xlabel('time [s]'), ylabel('CH1 sEMG [mV]')
% the rectified and filtered signal ('envelop')
fL=500;                         % low pass filter cut off [Hz]
fH = 20;                          % high pass filter cut off [Hz]
[b,a]=butter(2,[fH*2 fL*2]/Fs);   % filter
rRAW1=filtfilt(b,a,abs(RAW1));    % filtered rectified emg
plot(t,rRAW1,'b','LineWidth',2), box off

%% plot CH2
N2=length(RAW2);                  %number of RAW sEMG data point
n=0:N2-1;
t=n/Fs;
figure
plot (t,RAW2), box off, hold on, xlabel('time [s]'), ylabel('CH2 sEMG [mV]')
rRAW2=filtfilt(b,a,abs(RAW2));    % filtered rectified emg
plot(t,rRAW2,'r','LineWidth',2), box off

%% notch filter

F0 = 49.91;                      % notch frequency
Fn = Fs/2;                        % Nyquist frequency
freqRatio = F0/Fn;                % ratio of notch freq. to Nyquist freq.

notchWidth = 0.0001;               % width of the notch

% Compute zeros
notchZeros = [exp( sqrt(-1)*pi*freqRatio ), exp( -sqrt(-1)*pi*freqRatio )];

% Compute poles
notchPoles = (1-notchWidth) * notchZeros;

```

```

b = poly( notchZeros ); % Get moving average filter coefficients
a = poly( notchPoles ); % Get autoregressive filter coefficients

% filter signal rRAW
rRAW1 = filter(b,a,rRAW1);
rRAW2 = filter(b,a,rRAW2);

plot(t,rRAW1,'r','LineWidth',2), box off
plot(t,rRAW2,'r','LineWidth',2), box off

```

3. Plot power spectrum density (PSD)

```

%% plot PSD
Peel=periodogram(RAW1);
[Prr1,w]=periodogram(rRAW1);
f=w*Fs/(2*pi);%
t1=t(1:length(RAW1));
figure
subplot(221),
plot(t1,RAW1), box off, xlabel('time [s]'), ylabel('RAW sEMG [mV]')
subplot(222)
plot(t1,rRAW1), box off, xlabel('time [s]'), ylabel('filtered sEMG [mV]')
subplot(223),
loglog(f,Peel), box off, xlabel('frequency [Hz]'), ylabel('Amplitude [mV]')
subplot(224)
loglog(f,Prr1), box off, xlabel('frequency [Hz]'), ylabel('Amplitude [mV]')

Peel=periodogram(RAW2);
[Prr1,w]=periodogram(rRAW2);
f=w*Fs/(2*pi);
t2=t(1:length(RAW2));
figure
subplot(221),
plot(t2,RAW2), box off, xlabel('time [s]'), ylabel('RAW sEMG [mV]')
subplot(222)
plot(t2,rRAW2), box off, xlabel('time [s]'), ylabel('filtered sEMG [mV]')
subplot(223),
loglog(f,Peel), box off, xlabel('frequency [Hz]'), ylabel('Amplitude [mV]')
subplot(224)
loglog(f,Prr1), box off, xlabel('frequency [Hz]'), ylabel('Amplitude [mV]')

```

4. Plot MNF, MDF and MFPV

```

%% calculate MNF and MDF
%
p = 3;
Ng = p*Fs; % the length of each group
step = 0.5*Fs; % step is 1s

```

```

loop = fix ((N1-Ng)/step);           % step*loops + Ng - step <= N
for i = 0:loop;
    for j = 1:Ng
        x1(j) = RAW1(step*i+j);          % x is the p second data group
        x2(j) = RAW2(step*i+j);          % x is the p second data group
    end
    for j = 1:Ng
        rx1(j) = rRAW1(step*i+j);
        rx2(j) = rRAW2(step*i+j);
    end

    freq = meanfreq(rx1,Fs); %freq = meanfreq(x) estimates the mean
normalized frequency, freq, of the power spectrum of a time-domain signal,
x.
    %freq = meanfreq(x,fs) estimates the mean frequency in terms of the
sample rate, fs.
    z1(i+1) = freq;
    freq = medfreq(rx1,Fs);
    z4(i+1) = freq;

    freq = meanfreq(rx2,Fs); %MNF freq = meanfreq(x) estimates the mean
normalized frequency, freq, of the power spectrum of a time-domain signal,
x.
    %freq = meanfreq(x,fs) estimates the mean frequency in terms of the
sample rate, fs.
    z2(i+1) = freq;
    freq = medfreq(rx2,Fs); %MDF
    z3(i+1) = freq;

    [c, lags] = xcorr (rx1, rx2);      %correlation
    D = max(c);                      %find delay
    z(i+1) = D/Fs;
    [c, lags] = xcorr (rx2, rx1);
    D = max(c);
    w(i+1) = D/Fs;

end

t = [0:loop];
t = t*(step/Fs);
figure
subplot(211),
plot(t,z1), box off, hold on
xlabel('time [s]')
ylabel('CH1 MNF [Hz]')
p = polyfit(t,z1,4);
y = polyval(p,t);
plot(t,y,'LineWidth',2)
M = movmean(z1,8);
plot(t,M,'LineWidth',2)
hold on

subplot(212),
plot(t,z4), box off, hold on
xlabel('time [s]')
ylabel('CH1 MDF [Hz]')

p = polyfit(t,z4,4);
y = polyval(p,t);
plot(t,y,'LineWidth',2)

```

```

M = movmean(z4,8);
plot(t,M,'LineWidth',2)

hold on

t = [0:loop];
t = t*(step/Fs);
figure
subplot(211),
plot(t,z2), box off, hold on
xlabel('time [s]')
ylabel('CH2 MNF [Hz]')

p = polyfit(t,z2,4);
y = polyval(p,t);
plot(t,y,'LineWidth',2)
M = movmean(z2,8);
plot(t,M,'LineWidth',2)

hold on

subplot(212),
plot(t,z3), box off, hold on
xlabel('time [s]')
ylabel('CH2 MDF [Hz]')

p = polyfit(t,z3,4);
y = polyval(p,t);
plot(t,y,'LineWidth',2)
M = movmean(z3,8);
plot(t,M,'LineWidth',2)

hold on

figure
plot(t,z/Fs,'r'), box off, hold on
xlabel('time [s]')
ylabel('delay [s]')
title('delay vs. time')

p = polyfit(t,z,4);
y = polyval(p,t);
plot(t,y/Fs,'g','LineWidth',2)
% M = movmean(z,8);
% plot(t,M,'LineWidth',2)
hold on

figure
ab = 1./z; %velocity = length / time, length is constant
N = normalize(ab, 'scale', 'first');
plot(t,N,'r'), box off, hold on
xlabel('time [s]')
ylabel('Normalized MFPV')

```

```

title('MFPV vs. time')

p = polyfit(t,N,4);
y = polyval(p,t);
plot(t,y,'g','LineWidth',2)
% M = movmean(z,8);
% plot(t,M,'LineWidth',2)
hold on

figure
plot(t,w/Fs,'r'), box off, hold on
xlabel('time [s]')
ylabel('delay [s]')
title('delay vs. time')

p = polyfit(t,w,4);
y = polyval(p,t);
plot(t,y/Fs,'g','LineWidth',2)
% M = movmean(z,8);
% plot(t,M,'LineWidth',2)
hold on

figure
ab = 1./w;
N = normalize (ab, 'scale', 'first');
plot(t,N,'r'), box off, hold on
xlabel('time [s]')
ylabel('Normalized MFPV')
title('MFPV vs. time')

p = polyfit(t,N,4);
y = polyval(p,t);
plot(t,y,'g','LineWidth',2)
% M = movmean(z,8);
% plot(t,M,'LineWidth',2)
hold on

```